

Synthesis and Biological Evaluation of Cleistocaltone A, an Inhibitor of Respiratory Syncytial Virus (RSV)

Lorenz Wiese,^a Sophie M. Kolbe,^b Manuela Weber,^a Martin Ludlow^{*b} and Mathias Christmann^{*a}

The first chemical synthesis of the phloroglucinol meroterpenoid cleistocaltone A (**1**) is presented. This compound, previously isolated from *Cleistocalyx operculatus* was reported to show promising antiviral properties. Based on a modified biosynthesis proposal, a synthetic strategy was devised featuring an intramolecular Diels-Alder reaction and an epoxidation/elimination sequence to generate the allyl alcohol handle in the side chain. The route was successfully executed and synthetic Cleistocaltone A was evaluated against a contemporary RSV-A strain.

Introduction

Viral infections pose a significant economic burden and societal threat worldwide.^{1–3} The recent COVID-19 pandemic caused by severe acute respiratory syndrome coronavirus 2 (SARS-CoV-2) has starkly highlighted the risks posed by respiratory viruses to vulnerable populations and the urgent need for effective antivirals. Respiratory Syncytial Virus (RSV) is also a potent respiratory pathogen and is responsible for high levels of acute lower respiratory tract infections in infants, the elderly and immunocompromised adults.^{4,5} Despite the urgency, the current landscape of antiviral treatments is sparse, underscoring the critical need for further antiviral development.⁶ Natural products have a long and successful history as privileged starting points in the search for novel therapeutic approaches to counter infectious diseases.^{7–9} One effective strategy for navigating their vast chemical space is to deconvolute molecular compositions of herbal remedies described in traditional Chinese medicine (TCM), thus building upon a wealth of knowledge based on centuries of use.¹⁰ For example, the genus *Cleistocalyx*, belonging to the Myrtaceae family, comprises various plant species, some of which are used in Southeast Asia to create medicinal teas. *Cleistocalyx operculatus* (Roxb.) Merr. and Perry, a tree native to southern China, has been traditionally used to treat cold, fever, and inflammation with extracts from its buds and leaves.¹¹ Cleistocaltone A (**1**, Figure 1), a polymethylated phloroglucinol meroterpenoid (PPM) isolated from the buds of *C. operculatus* by Ye, Wang, and co-workers in 2019, was demonstrated to possess promising *in vitro* activity against RSV.¹²

In nature, components from diverse classes of natural products frequently merge to form compounds with novel biological activities. Among these classes, phloroglucinol meroterpenoids stand out.¹³ These compounds consist of a phloroglucinol segment and a terpene segment. The terpene portion typically originates from a geranyl group, which undergoes a series of biosynthetic transformations involving oxidation and cyclization. For instance, elodeidol G (**2**, Figure 1), an anti-inflammatory agent isolated by Luo, Kong, and coworkers, features a terpene moiety proposed to be biosynthesized from an oxidized geranyl building block through a series of epoxidations and an acid-catalyzed epoxide opening cascade.¹⁴ Similarly, the cytotoxic compound hyphenrone J (**3**, Figure 1), isolated by Qin, Xu, and coworkers, contains two prenyl groups and an oxidized geranyl side chain.¹⁵

Biosynthetically, the phloroglucinol portion of cleistocaltone A (**1**) is proposed to originate from champanone B (**4**, Figure 1). Addition of geranyl pyrophosphate (GPP, **5**) then forms geranyl champanone B **6**. Subsequent desaturation of the geranyl terminus and isomerization of the homobenzylic double bond generates a triene, enabling an intramolecular Diels-Alder cycloaddition (IMDA) with the cinnamoyl dienophile.

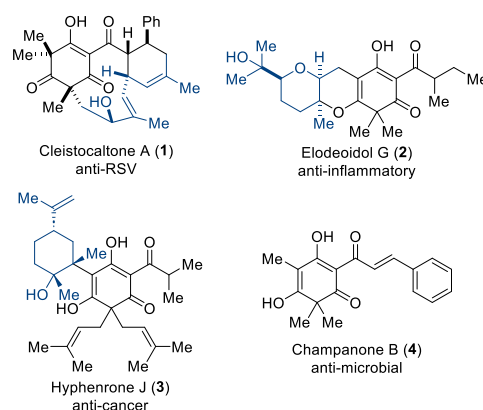
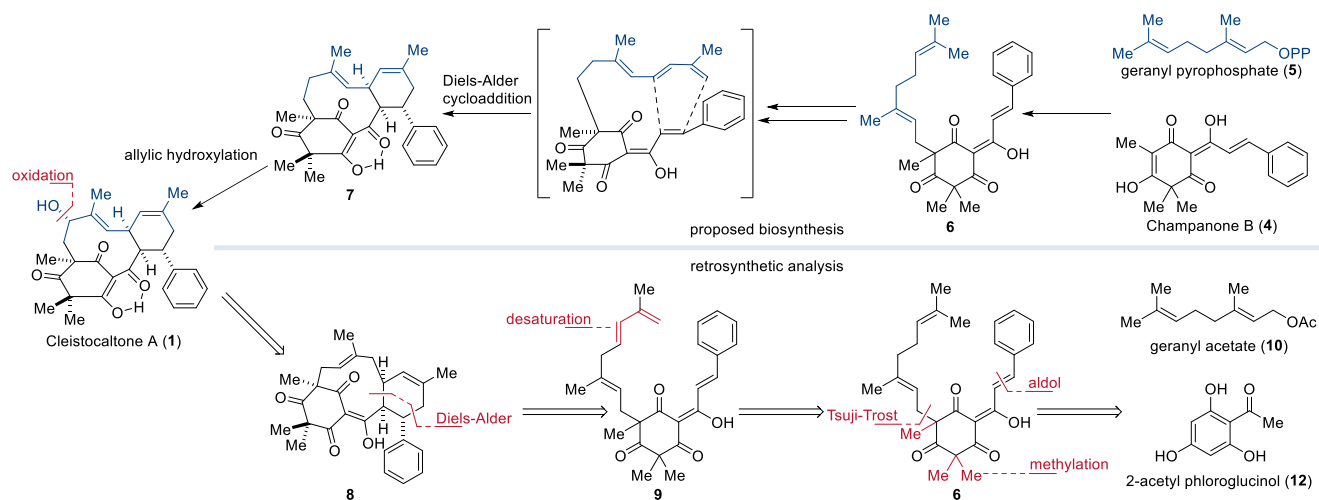


Figure 1 Example for different phloroglucinol meroterpenoids with various biological activities.^{12,14–16}

^a Institute of Chemistry and Biochemistry, Freie Universität Berlin, 14195 Berlin, Germany

^b Research Center for Emerging Infections and Zoonoses, University of Veterinary Medicine Hannover Foundation, 30559 Hannover, Germany



Scheme 1 Biosynthesis of cleistocaltone A (**1**) proposed by Ye, Wang, and coworkers and retrosynthetic analysis both featuring an IMDA as the key step.¹²

This reaction forges the characteristic 10-membered macrocycle found in **7** (Scheme 1).¹² Ye, Wang, and coworkers succeeded in isolating 24 mg of (\pm)-cleistocaltone A (**1**) from 15 kg of plant material, highlighting the scarcity of this compound from biological sources.¹² This underlines the significance of chemical synthesis to produce substantial quantities of (\pm)-cleistocaltone A (**1**) for further biological evaluation.

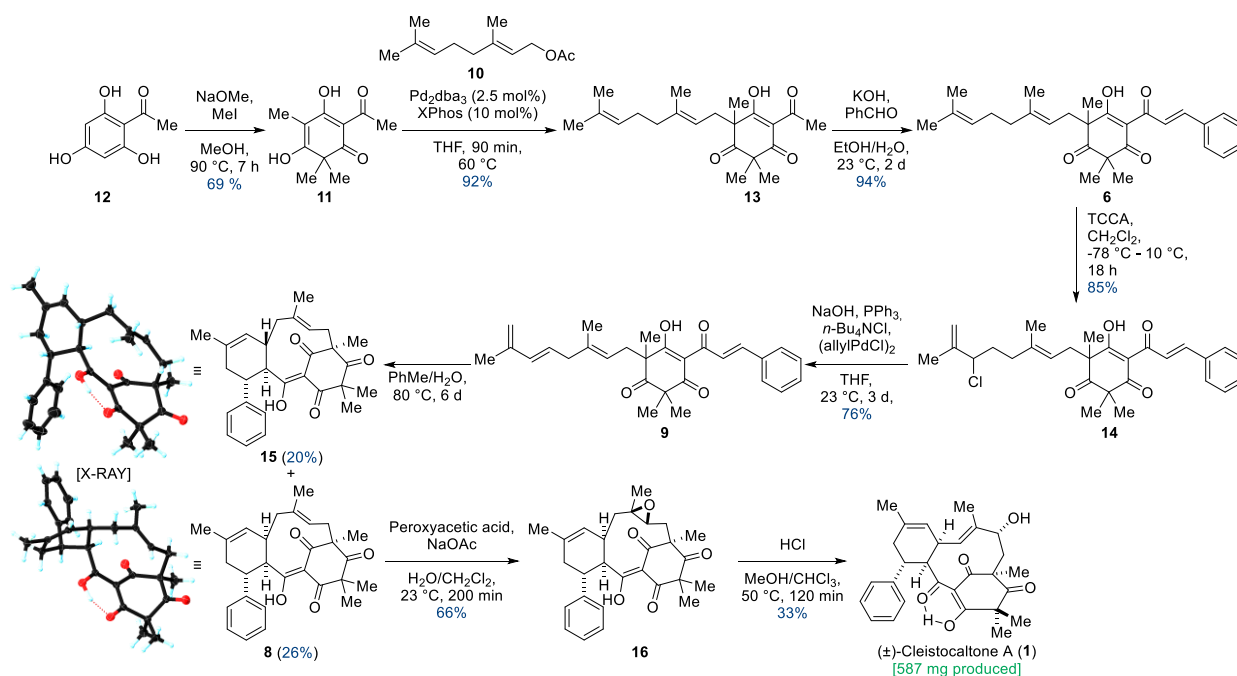
In recent years, biomimetic strategies have emerged as an intriguing and efficient approach for synthesizing complex natural products. These strategies elegantly mimic the pathways found in nature.^{17–19} By harnessing the innate reactivity of molecules, biomimetic syntheses often minimize the need for protection groups, resulting in greater efficiency and sustainability.²⁰

Mirroring the proposed biosynthetic pathway, we envisioned an IMDA as the pivotal step for constructing the 10-membered

macrocycle of **8**. To generate the diene moiety in **9** for the IMDA, we planned a selective desaturation at the terminus of the geranyl group in **6**, obtained from geranyl acetate (**10**). This geranyl unit would be attached to the nucleophilic carbon atom of methylated phloroglucinol **11** using a Tsuji-Trost alkylation.²¹ The phloroglucinol building block would be synthesized from commercially available 2-acetyl phloroglucinol (**12**) through trimethylation and an aldol condensation.

Results and Discussion

Our synthesis, as outlined in Scheme 2, commenced with the trimethylation of 2-acetyl phloroglucinol (**12**), employing sodium methoxide and methyl iodide.



Scheme 2 Linear synthesis of cleistocaltone A (**1**) starting from 2-acetyl phloroglucinol (**12**) and geranyl acetate (**10**).

Following the neutralization of the reaction mixture, the desired product precipitated, allowing for straightforward separation via filtration. This workup efficiently removed impurities and byproducts, including dimethylated 2-acetyl phloroglucinol, which stayed in solution. Consequently, we obtained trimethylated acetyl phloroglucinol **11** with a yield of 69%. The obtained trimethylated acetyl phloroglucinol **11** was then coupled with commercially available geranyl acetate (**10**) in a Tsuji-Trost allylic alkylation. Using Pd₂dba₃ as a Pd(0) source and testing multiple ligands, XPhos proved superior, yielding the geranylated phloroglucinol **13** with an excellent yield of 92%. Rendering the coupling reaction enantioselective would be highly desirable. The single stereocenter formed in the Tsuji-Trost reaction ultimately dictates whether (+)- or (-)-cleistocaltone A (**1**) is synthesized due to the diastereoselectivity of subsequent steps. Unfortunately, despite rigorous screening, we could not identify a chiral ligand that induced significant enantiomeric excess. Consequently, we proceeded with the synthesis using a racemic mixture of geranylated acetyl phloroglucinol **13**.

In the subsequent aldol condensation, **13** was reacted with benzaldehyde under basic conditions. Due to a competing Cannizzaro reaction consuming benzaldehyde (yielding benzyl alcohol and benzoic acid), a portion-wise addition of 6 equivalents of aldehyde was crucial for complete conversion. Then the high solubility of **6** in cyclohexane was exploited for extraction, leaving benzoic acid and much of the benzyl alcohol in the aqueous phase. Unreacted benzaldehyde was removed under high vacuum, greatly streamlining the purification process. This yielded geranyl champanone B **6** in 94% yield.

The terminus of the geranyl moiety in **6** was selectively chlorinated using trichloroisocyanuric acid (TCCA) in CH₂Cl₂, with careful temperature control being crucial. While the reaction proceeded smoothly on a milligram scale (85% yield of **14**, simple filtration), scaling up to gram quantities significantly decreased the yield to 50% and complicated the column chromatography purification due to increased side-product formation.

In the subsequent step, the allylic chloride in **14** was eliminated via a palladium-catalyzed β -hydride elimination to afford diene **9** in 76% yield. The combination of sodium hydroxide and the phase-transfer catalyst tetrabutylammonium chloride ensured efficient removal of the liberated hydrochloric acid (HCl).²²

With the required structural elements assembled, a thermal IMDA was performed in a biphasic mixture of water and toluene. This process afforded diastereomers **15** and **8** in 20% and 26% yields, respectively. Crystallization proved to be the most efficient purification method. Treatment of the crude product with a pentane followed by cyclohexane preferentially dissolved the undesired IMDA diastereomer **15**, leaving the desired diastereomer **8** as a solid. While this purification was extremely convenient, some amount of **8** also dissolved, resulting in a reduced yield of only 26% (compared to a possible 32% as determined by ¹H-NMR). The absolute configurations of **8** and **15** were confirmed by XRD analysis.

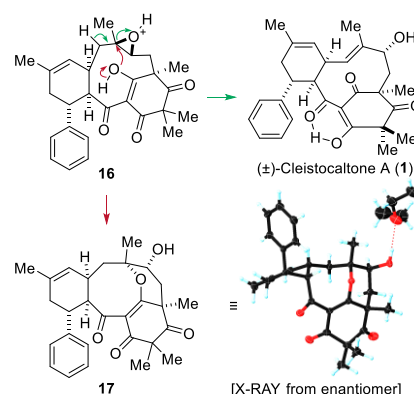
In exploring the impact of various solvents on the IMDA reaction's diastereomeric ratio, a 3:1 excess of the undesired

diastereomer **15** was observed in both pyridine and *n*-butanol. Unfortunately, no other tested solvent yielded an excess of the desired diastereomer **8**. Consequently, a toluene/water mixture was chosen, allowing the reaction to proceed at a lower temperature (80 °C), which minimized side product formation and simplified purification.

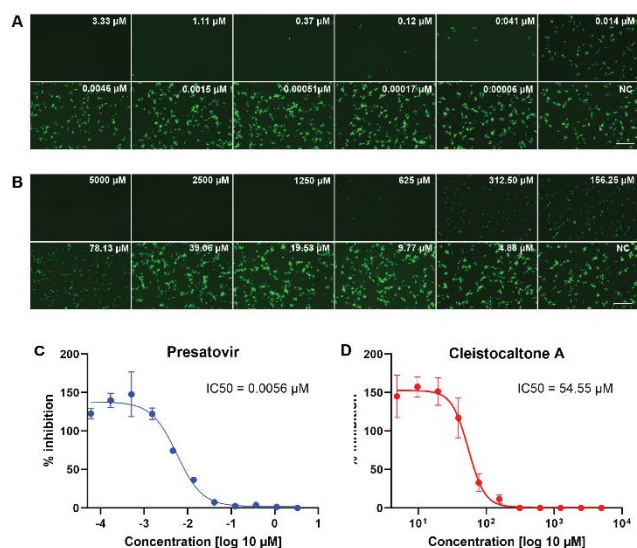
The epoxidation of **8** presented a challenge, as its two trisubstituted double bonds appeared electronically similar. We speculated that strain-release in the transition state would render the macrocyclic double bond significantly more reactive. The facial preference was predicted from the X-ray crystal structure of the starting material. Treatment of **8** with peroxyacetic acid in a biphasic sodium acetate/dichloromethane mixture selectively furnished epoxide **16** as a single diastereomer in 66% yield.

Various conditions for opening epoxide **16** were investigated. Lewis acidic conditions generally led to decomposition. Basic conditions, even using strong bases such as *n*-butyl lithium at room temperature, resulted in no conversion. This lack of reactivity is attributed to steric hindrance, with the macrocycle shielding the acidic α -position adjacent to the epoxide. Fortunately, Brønsted acidic conditions proved successful. Treatment with HCl at 50 °C opened the epoxide, yielding the allylic alcohol and, ultimately, cleistocaltone A (**1**) in a 33% yield. Additionally, the acid-mediated opening of the epoxide in **16** resulted in an intriguing side product **17**, characterized by an unusual tetracyclic structure that includes an eight-membered cyclic ether. The structure was confirmed through XRD analysis. It is proposed that this product originates from a nucleophilic attack by the enol-oxygen on the tertiary carbon center, a process initiated by the protonation of the epoxide (Scheme 3).

We investigated the antiviral efficacy of synthetic cleistocaltone A (**1**) against a contemporary recombinant RSV-A strain (0594, genotype ON1)²³ using an *in vitro* model system (Scheme 4). Presatovir, a known selective and potent inhibitor of RSV-induced cell fusion,²⁴ served as a positive control. We confirmed Presatovir's high antiviral efficacy in infected Vero cells, with an IC₅₀ of 0.0056 μ M. Cleistocaltone A (**1**) also inhibited RSV infection, with a modestly higher IC₅₀ of 54.55 μ M.



Scheme 3 Proposed mechanism for the formation of cleistocaltone A (**1**) via an acid mediated epoxide opening and cyclic ether **17** via a nucleophilic attack of the enol-OH in epoxide **16**.



Scheme 4 Assessment of the antiviral efficacy of cleistocaltone A (**1**) against RSV. (A-B) Vero cells were pretreated with three-fold serial dilutions of the fusion inhibitor Presatovir or two-fold serial dilutions of cleistocaltone A (**1**) and infected with rSV-A-0594-EGFP (2000 TCID₅₀/well) in the presence of each compound. Fluorescence photomicrographs showing EGFP fluorescence were obtained by UV microscopy at 48 hours post-infection. Scale bars, 500 μm. (C-D) Quantification of EGFP fluorescence in drug treated Vero cells was performed in 4% PFA fixed cells at 48 h.p.i. using a Tecan Infinite 2000 plate reader and normalized to untreated controls wells containing 0.1% DMSO. IC₅₀ values were determined by nonlinear regression analysis using GraphPad Prism 10. Error bars represent the standard deviations from two independent experiments (n=8).

Although the IC₅₀ of synthetic cleistocaltone A (**1**) is roughly tenfold higher than that of the isolated compound (IC₅₀ = 6.75 ± 0.75 μM),¹² it remains within a relevant range.

Conclusion and Outlook

We successfully executed a biomimetic gram-scale synthesis of cleistocaltone A (**1**) using an efficient eight-step route with an overall yield of 2.2%. Our approach enables further derivatization at various stages to obtain synthetic analogues for structure-activity-relationship (SAR) studies, paving the way for potential drug development.

Author Contributions

M.C. supervised the project. L.W. developed the synthesis and carried out all synthetic experiments. M.L. and S.K. developed and conducted all biological testing. M.W. performed all XRD measurements. L.W., M.C., and M.L. wrote the manuscript.

Conflicts of interest

There are no conflicts to declare.

Acknowledgements

The authors acknowledge the assistance of the Core Facility BioSupraMol supported by the DFG and Kristin Laudeley for excellent technical support.

Notes and references

- 1 T. Szucs, *J. Antimicrob. Chemother.*, 1999, **44**, 11–15.
- 2 H. Bolek, L. Ozisik, Z. Caliskan and M. D. Tanriover, *J. Med. Virol.*, 2022, 95:e28153.
- 3 A. M. Fendrick, A. S. Monto, B. Nightengale and M. Sarnes, *Arch. Intern. Med.*, 2003, **163**, 487–494.
- 4 M. Savic, Y. Penders, T. Shi, A. Branche and J. Y. Pirçon, *Influenza Other Respi. Viruses*, 2022, 1–10.
- 5 P. Srikanthiah, P. Vora and K. P. Klugman, *Clin. Infect. Dis.*, 2021, **73**, S177–S179.
- 6 A. C. Langedijk and L. J. Bont, *Nat. Rev. Microbiol.*, 2023, **21**, 734–749.
- 7 G. M. Cragg and D. J. Newman, *Biochim. Biophys. Acta - Gen. Subj.*, 2013, **1830**, 3670–3695.
- 8 T. Rodrigues, D. Reker, P. Schneider and G. Schneider, *Nat. Chem.*, 2016, **8**, 531–541.
- 9 A. L. Harvey, *Drug Discov. Today*, 2008, **13**, 894–901.
- 10 O. Fidan, J. Ren and J. Zhan, *World J. Tradit. Chinese Med.*, 2022, **8**, 59–76.
- 11 C. Wang, P. Wu, S. Tian, J. Xue, L. Xu, H. Li and X. Wei, *J. Nat. Prod.*, 2016, **79**, 2912–2923.
- 12 J. G. Song, J. C. Su, Q. Y. Song, R. L. Huang, W. Tang, L. J. Hu, X. J. Huang, R. W. Jiang, Y. L. Li, W. C. Ye and Y. Wang, *Org. Lett.*, 2019, **21**, 9579–9583.
- 13 M. Nazir, M. Saleem, M. I. Tousif, M. A. Anwar, F. Surup, I. Ali, D. Wang, N. Z. Mamadaliyeva, E. Alshammari, M. L. Ashour, A. M. Ashour, I. Ahmed, Elizbit, I. R. Green and H. Hussain, *Biomolecules*, 2021, **11**, 1–61.
- 14 Q. J. Li, P. F. Tang, X. Zhou, W. J. Lu, W. J. Xu, J. Luo and L. Y. Kong, *Bioorg. Chem.*, 2020, **104**, 104275.
- 15 X. W. Yang, M. M. Li, X. Liu, D. Ferreira, Y. Ding, J. J. Zhang, Y. Liao, H. B. Qin and G. Xu, *J. Nat. Prod.*, 2015, **78**, 885–895.
- 16 A. Bonilla, C. Duque, C. Garzón, Y. Takaishi, K. Yamaguchi, N. Hara and Y. Fujimoto, *Phytochemistry*, 2005, **66**, 1736–1740.
- 17 A. J. E. Novak, C. E. Grigglesstone and D. Trauner, *J. Am. Chem. Soc.*, 2019, **141**, 15515–15518.
- 18 T. V. de Castro, D. M. Huang, C. J. Sumby, A. L. Lawrence and J. H. George, *Chem. Sci.*, 2023, **14**, 950–954.
- 19 S. A. French, C. J. Sumby, D. M. Huang and J. H. George, *J. Am. Chem. Soc.*, 2022, **144**, 22844–22849.
- 20 R. Bao, H. Zhang and Y. Tang, *Acc. Chem. Res.*, 2021, **54**, 3720–3733.
- 21 B. M. Trost, *Tetrahedron*, 2015, **71**, 5708–5733.
- 22 European Patent Office, EP 1 072 589 A2, 2001, 11–12.
- 23 W. K. Jo, A. Schadenhofer, A. Habierski, F. K. Kaiser, G. Saletti, T. Ganzenmueller, E. Hage, S. Haid, T. Pietschmann, G. Hansen, T. F. Schulz, G. F. Rimmelzwaan, A. D. M. E. Osterhaus and M. Ludlow, *Proc. Natl. Acad. Sci. U. S. A.*, 2021, **118**, e2026558118.
- 24 J. P. DeVincenzo, R. J. Whitley, R. L. Mackman, C. Scaglioni-Weinlich, L. Harrison, E. Farrell, S. McBride, R. Lambkin-Williams, R. Jordan, Y. Xin, S. Ramanathan, T. O’Riordan, S. A. Lewis, X. Li, S. L. Toback, S.-L. Lin and J. W. Chien, *N. Engl. J. Med.*, 2014, **371**, 711–722.

Synthesis and Biological Evaluation of Cleistocaltone A

Lorenz Wiese,^a Sophie Kolbe,^b Manuela Weber,^a Martin Ludlow*^b and Mathias Christmann*^a

^aInstitute of Chemistry and Biochemistry, Freie Universität Berlin, 14195 Berlin, Germany.

^bResearch Center for Emerging Infections and Zoonoses, University of Veterinary Medicine
Hannover Foundation, 30559 Hanover, Germany.

*E-Mail: m.christmann@fu-berlin.de

Supporting Information

Table of Contents

1. General Information	1
1.1 Materials and Methods	1
1.2 Analysis	1
1.3 Antiviral Inhibition Assay	2
2. Scheme 1: Linear Route to Intermediate 9	3
3. Scheme 2: Convergent Route to Intermediate 9	3
4. Scheme 3: IMDA and Backbone Oxidation	4
5. Table 1: Ligand Screening for the Enantioselective Tsuji-Trost Coupling of Geranyl Acetate (10) and Trimethylated Phloroglucinol 12	4
6. Figure 1: Structures of Chiral Ligands from Solvias Asymmetric Screening Kit^[6]	5
7. Table 2: Solvent Screening for the IMDA	6
8. Experimental Procedures and Analytical Data	7
8.1 Linear Route to Intermediate 9	7
8.2 Convergent Route to Intermediate 9	13
8.3 IMDA and Backbone Oxidation	17
9. Comparison of NMR Data	22
9.1 (±)-Cleistocaltone A (1)	22
10. X-ray data	23
10.1 IMDA-diastereomer 15	23
10.2 IMDA-diastereomer 8	24
10.3 Sideproduct 17	25
11. NMR Spectra	26
12. References	39

1. General Information

1.1 Materials and Methods

Reactions with air or moisture sensitive substances were carried out under an argon atmosphere using standard Schlenk technique. Ambient or room temperature (RT) refers to 18–23 °C. Heating of reactions was performed with an oil bath unless otherwise noted. “Brine” refers to a sat. aq. NaCl solution.

Unless otherwise noted, all starting materials and reagents were purchased from commercial distributors and used without further purification. Anhydrous dichloromethane and tetrahydrofuran were provided by purification with a MBraun SPS-800 solvent system (BRAUN) using solvents of HPLC grade purchased from FISHER Scientific and ROTH. 2-Acetyl phloroglucinol monohydrate was dried for 16 h at 60 °C in the high vacuum to obtain dry 2-acetyl phloroglucinol which was stored under argon. Solvents for extraction, crystallization and flash column chromatography were purchased in technical grade and distilled under reduced pressure prior to use.

Column chromatography was performed on silica 60 M (0.040-0.063 mm, 230-400 mesh, MACHEREY-NAGEL).

Medium pressure liquid chromatography (MPLC) was performed with a TELEDYNE ISCO Combi-Flash Rf200 using prepacked silica columns and cartridges from TELDYNE. UV response was monitored at 254 nm and 280 nm. As eluents, cyclohexane (99.5+% quality) and EtOAc (HPLC grade) were used.

1.2 Analysis

Reaction monitoring: Reactions were monitored by thin layer chromatography (TLC). TLC-analysis was performed on silica gel coated aluminium plates ALUGRAM® Xtra SIL G/UV₂₅₄ purchased from MACHEREY-NAGEL. Products were visualized by UV light at 254 nm and by using staining reagents (based on KMnO₄, Ce(SO₄)₂ and anisaldehyde).

NMR spectroscopy: ¹H NMR and ¹³C NMR spectral data were recorded on JEOL (ECX 400, ECP 500), VARIAN (Inova 600) and BRUKER (AVANCE III 500, AVANCE III 700) spectrometers in the reported deuterated solvents. The chemical shifts (δ) are listed in parts per million (ppm) and are reported relative to the corresponding residual non-deuterated solvent signal (CDCl₃: δ_H = 7.26 ppm, δ_C = 77.2 ppm; CD₂Cl₂: δ_H = 5.32 ppm, δ_C = 53.8 ppm; DMSO-*d*₆: δ_H = 2.50 ppm, δ_C = 39.5 ppm). Integrals are in accordance with assignments; coupling

constants (*J*) are given in Hz. Multiplicity is indicated as follows: s (singlet), d (doublet), t (triplet), q (quartet), p (pentet), br (broad) and combinations thereof. In the case where no multiplicity could be identified, the chemical shift range of the signal is given as m (multiplet). ¹³C NMR spectra are ¹H-broadband decoupled.

High resolution mass spectrometry: High resolution mass spectra (HRMS) were measured with an AGILENT 6210 ESI-TOF (10 μL/min, 1.0 bar, 4 kV) instrument.

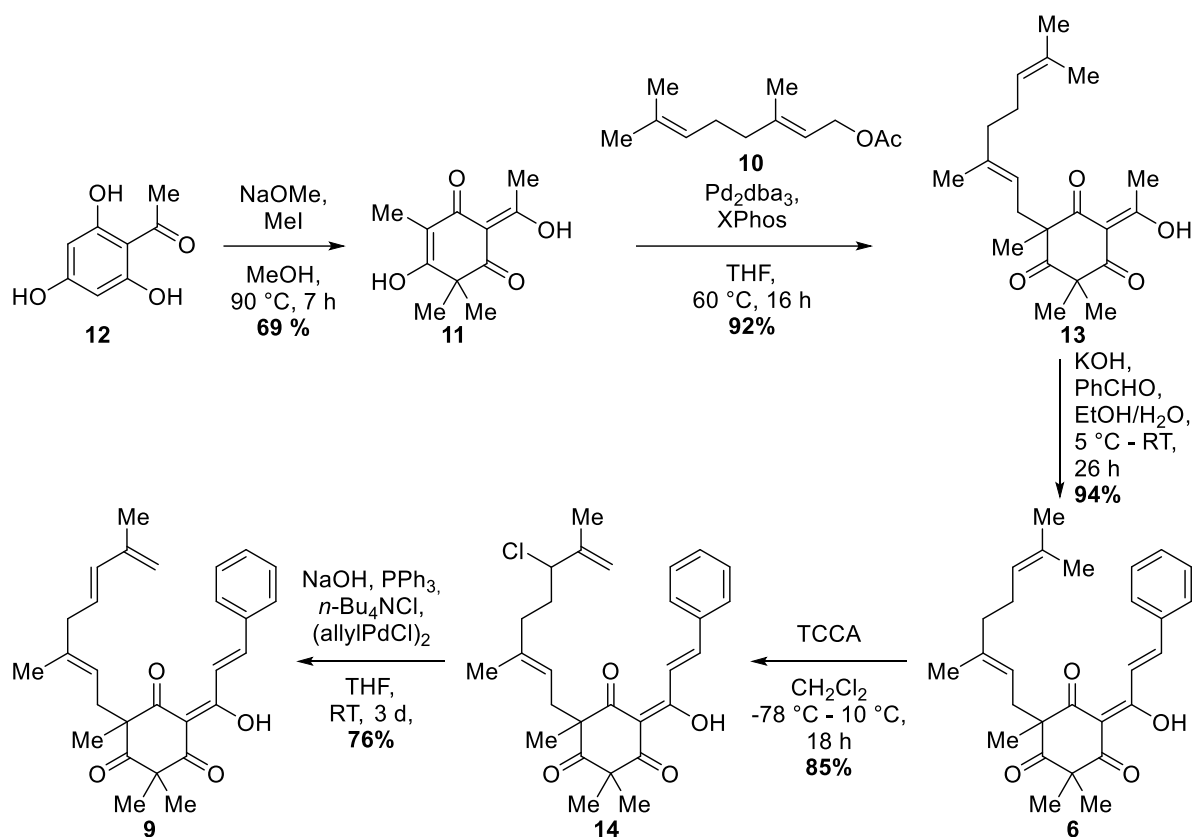
Infrared spectroscopy: Infrared (IR) spectra were measured on a Jasco FT/IR-4100 Type A spectrometer with a TGS detector. Wavenumbers $\tilde{\nu}$ are given in cm⁻¹.

X-ray: X-ray diffraction data was collected on a BRUKER D8 Venture CMOS area detector (Photon 100) diffractometer with Cu K α radiation. Single crystals were coated with perfluoroether oil and mounted on a 0.2 mm Micromount. The structures were solved with the ShelXT¹ structure solution program using intrinsic phasing and refined with the ShelXL² refinement package using least squares on weighted F² values for all reflections using OLEX2.³

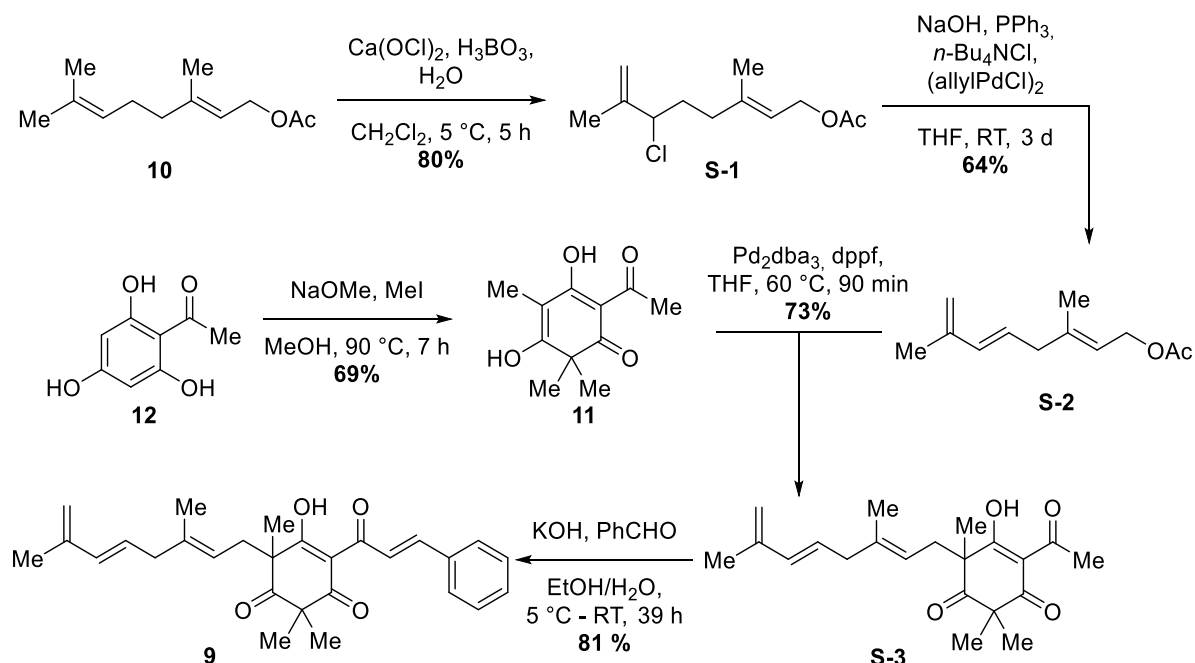
1.3 Antiviral Inhibition Assay

Vero and HEp-2 cells were cultured in Dulbecco's modified Eagle's medium (Thermo Fisher Scientific) supplemented with 10% fetal bovine serum (FBS), 1% penicillin/streptomycin, and 1% GlutaMAX and were cultured at 37 °C with 5% CO₂. Working stocks of rRSV-A-0594-EGFP, a recombinant respiratory syncytial virus (RSV) strain based on a contemporary subtype A strain, were generated, and titrated on HEp-2 cells as previously described.⁴ Presatovir (GS-5806) was purchased from MedChemExpress and has been previously shown to act as an RSV fusion inhibitor.⁵ Stock solutions of Cleistocaltone A (10 mM) and Presatovir (1 mM) were prepared in dimethyl sulfoxide (DMSO) (Sigma Aldrich), aliquoted and stored at -20 °C and -80 °C respectively. Vero cells grown in 96 well trays were pre-treated with either three-fold serial dilutions of Cleistocaltone A (**1**) or two-fold serial dilutions of Presatovir in Opti-MEM (Thermo Fisher Scientific) prior to infection with 2000 TCID₅₀/well of rRSV-A-0594-EGFP. Cells were incubated at 37 °C for 48 hours and inhibition of infection was assessed by visualization of EGFP fluorescence using UV microscopy. Cells were fixed in 4% (w/v) paraformaldehyde and the fluorescence quantified using a Tecan Infinite 2000 plate reader. The resulting values were normalized to rRSV-A-0594-EGFP infected Vero cells containing 0.1% dimethyl sulfoxide DMSO and are shown as the mean (n=8) of two biological replicates. IC₅₀ values were determined by nonlinear regression analysis using GraphPad Prism 10.

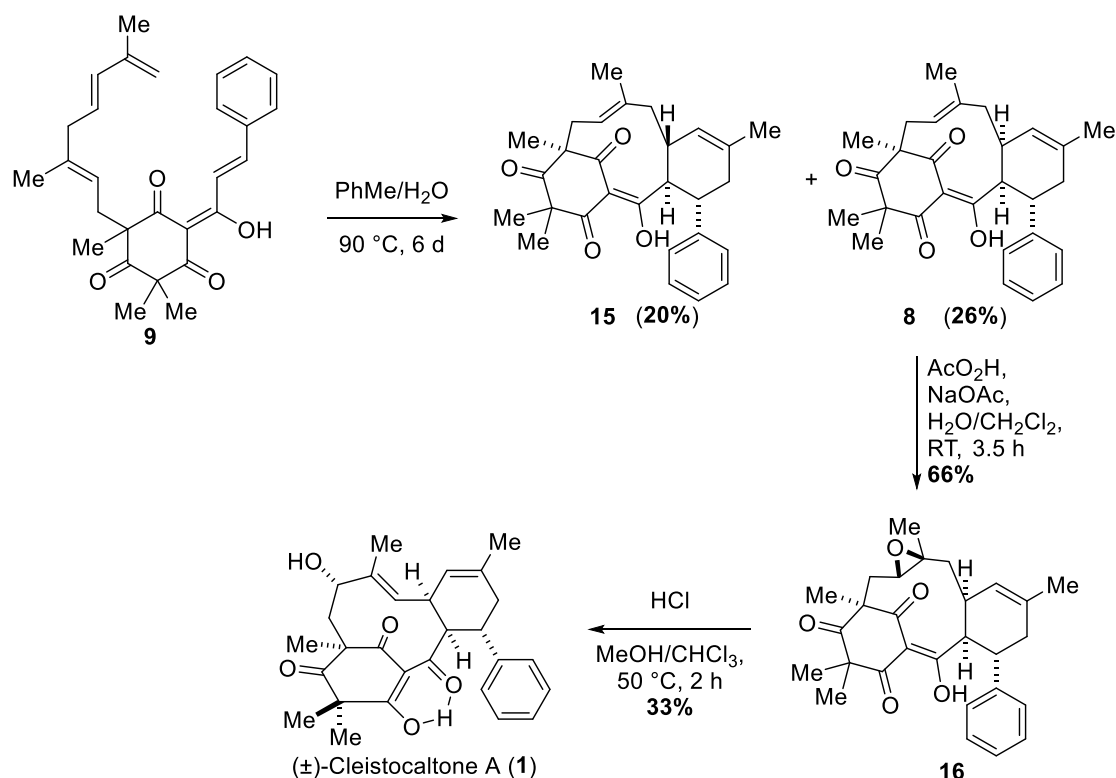
2. Scheme 1: Linear Route to Intermediate 9



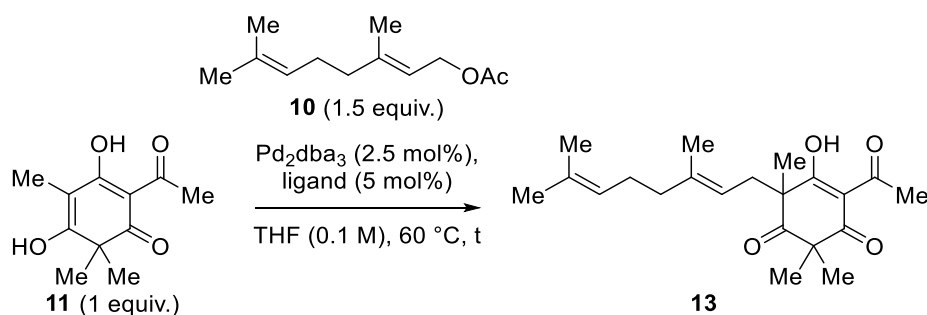
3. Scheme 2: Convergent Route to Intermediate 9



4. Scheme 3: IMDA and Backbone Oxidation



5. Table 1: Ligand Screening for the Enantioselective Tsuji-Trost Coupling of Geranyl Acetate (10) and Trimethylated Phloroglucinol 11

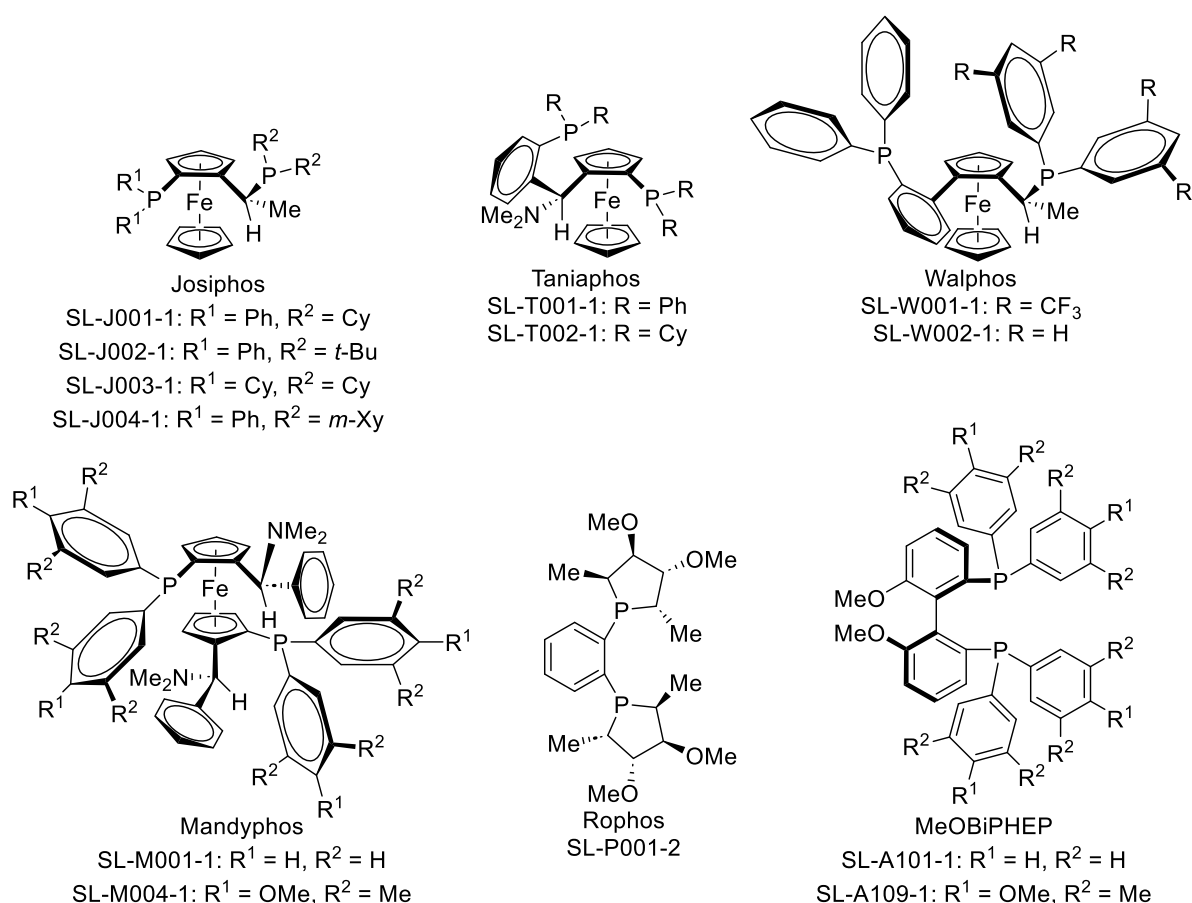


Entry	Ligand ^a	t (h)	Yield	ee ^b	Comment
1	(<i>R</i>)-BINAP	48	-	-	no conversion
2	DuPhos	48	-	-	no conversion
3	(<i>R, R</i>)-DACH-Trost-Ligand	36	22%	0%	
4	Josiphos-SL-J001-1	16	-	-	no conversion
5	Josiphos-SL-J002-1	16	-	-	no conversion
6	Josiphos-SL-J003-1	16	-	-	no conversion

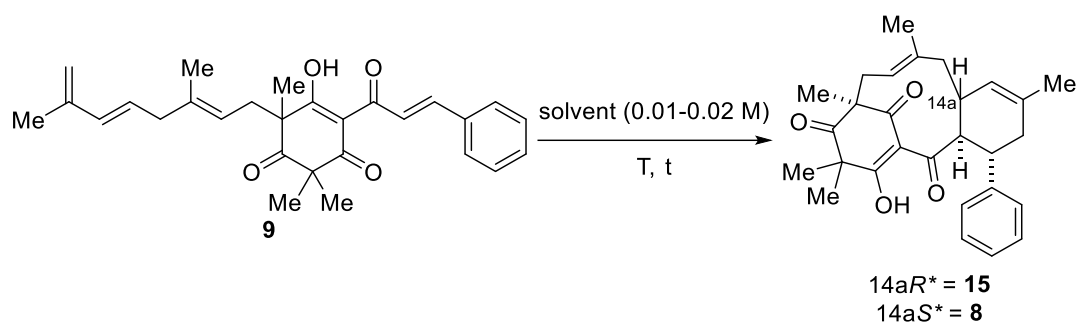
7	Josiphos-SL-J005-1	16	-	-	no conversion
8	Taniaphos-SL-T001-1	16	-	-	no conversion
9	Taniaphos-SL-T002-1	16	-	-	no conversion
10	Walphos-SL-W001-1	16	12%	0%	-
11	Walphos-SL-W002-1	16	55%	0%	-
12	Mandyphos-SL-M001-1	16	61%	0%	-
13	Mandyphos-SL-M004-1	16	44%	0%	-
14	Rophos-SL-P001-2	16	-	-	no conversion
15	MeOBIPHEP-SL-A-101-1	16	-	-	no conversion
16	MeOBIPHEP-SL-A-109-1	16	-	-	no conversion

a) All ligands except for (*R*)-BINAP, Duphos and (*R,R*)-DACH-Trost-Ligand were used from Solvias Asymmetric Ligands Screening Kit.⁶ b) All *ee* were determined by NP-HPLC using a Chiralpak IC column. The eluent consisted of 0.5% *iso*-propanol in *n*-hexane with a flow rate of 0.5 mL/min. The retention times for both enantiomers were 10.7 min and 11.5 min, respectively.

6. Figure 1: Structures of Chiral Ligands from Solvias Asymmetric Screening Kit⁶



7. Table 2: Solvent Screening for the IMDA



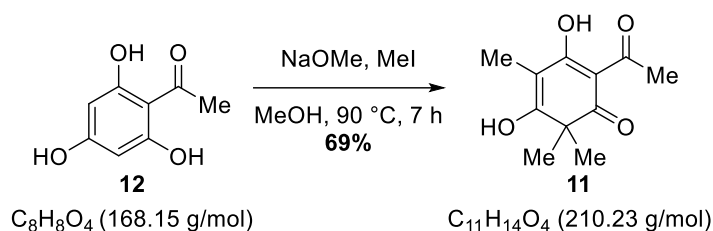
Entry	Solvent	t (d)	T (°C)	<i>dr</i> (15:8) ^a	Comment
1 ^b	ethanol/water	4	110	5:2	-
2 ^b	<i>n</i> -butanol	4	110	3:1	-
3 ^b	<i>tert</i> -butanol	4	110	5:4	-
4 ^b	pyridine	5	120	3:1	significant decomposition
5 ^b	tetrahydrofuran	1	110	5:4	significant decomposition
6 ^b	methyltetrahydrofuran	1	110	4:3	significant decomposition
7 ^b	1,4-dioxane	5	120	5:4	-
8 ^b	1,2-dimethoxyethane	1	110	4:3	-
9 ^b	diglyme	5	120	4:3	-
10 ^b	1,2-dichloroethane	1	110	4:3	-
11 ^b	benzotrifluoride	5	120	10:7	-
12 ^b	chlorobenzene	5	120	5:3	-
13 ^b	toluene	5	110	10:7	-
14 ^b	heptane	5	120	10:7	-
15	toluene/water	5	90	3:2	very facile purification

a) All *dr* were determined by crude ¹H-NMR using the integrals of the enol-O-H at 17.50 ppm for **15** and 17.96 ppm for **8**. b) Reaction was carried out in a capped vial.

8. Experimental Procedures and Analytical Data

8.1 Linear Route to Intermediate 9

8.1.1 2-Acetyl-3,5-dihydroxy-4,6,6-trimethylcyclohexa-2,4-dien-1-one (11)



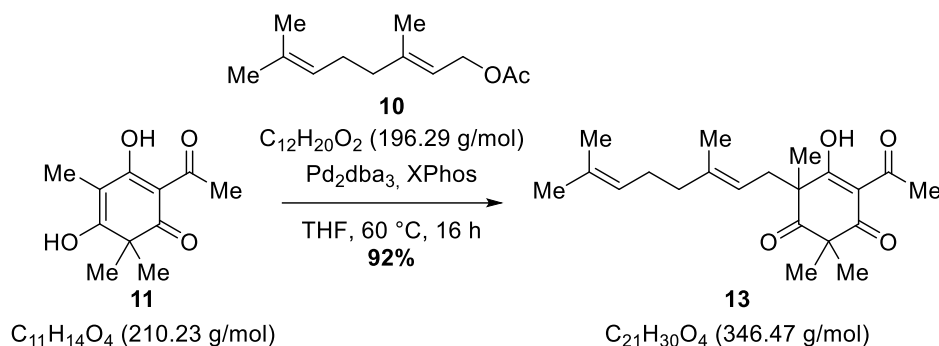
Sodium (7.59 g, 330 mmol, 3.7 equiv.) was added to dry methanol (250 mL) in a three-necked round-bottom flask equipped with a reflux-condenser. After the sodium had reacted completely, 2-acetylphloroglucinol (**12**, 15.0 g, 89.2 mmol, 1.0 equiv.) dissolved in dry methanol (200 mL) was added slowly. Afterwards, methyl iodide (18.2 mL, 41.8 g, 294 mmol, 3.3 equiv.) was added slowly. Then, the mixture was heated to 90 °C and stirred at this temperature for 7 h. Afterwards, the mixture was cooled down to 5 °C using an ice/water-bath. The mixture was acidified to pH = 2-3 with 1 M aq. HCl. The precipitated solid was filtered off, washed with water and dried under high vacuum. Trimethylated acetyl phloroglucinol **11** (12.9 g, 61.6 mmol, 69%) was isolated as an off-white powder and used without further purification.

1H NMR (600 MHz, DMSO- d_6): δ = 18.96 (s, 1H), 2.46 (s, 3H), 1.77 (s, 3H), 1.27 (s, 6H) ppm.

^{13}C NMR (151 MHz, DMSO- d_6): δ = 199.4, 196.0, 188.9, 176.0, 105.1, 101.9, 48.2, 27.8, 24.3, 7.2 ppm.

The spectroscopic data are in accordance with the literature.⁷

8.1.2 4-Acetyl-6-(3,7-dimethylocta-2,6-dien-1-yl)-5-hydroxy-2,2,6-trimethylcyclohex-4-ene-1,3-dione (**13**)



A Schlenk flask was loaded with trimethylated acetyl-phloroglucinol **11** (11.78 g, 56.0 mmol, 1.0 equiv.), $\text{Pd}_2(\text{dba})_3$ (1.28 g, 1.40 mmol, 2.5 mol%) and XPhos (2.67 g, 5.60 mmol, 10 mol%). The flask was evacuated and backfilled with argon three times. Afterwards, dry THF (500 mL) and geranyl acetate (**10**, 18.1 mL, 16.5 g, 84.1 mmol, 1.5 equiv.) were added subsequently and the mixture was heated to 60 °C. After stirring at this temperature for 16 h, the mixture was allowed to cool down to RT and filtered through a plug of silica. The silica was thoroughly rinsed with CH_2Cl_2 . The filtrate was concentrated under reduced pressure and the crude product was purified by column chromatography (SiO_2 , EtOAc:pentane/2% to 5%) to afford geranylated acetyl phloroglucinol **13** (17.8 g, 51.4 mmol, 92%) as a yellowish oil.

The product was isolated as a mixture of two interconverting tautomers (tautomer A : tautomer B = 1:0.7) which gave two sets of signals in the ^1H - and ^{13}C -NMR in which many signals overlapped.

Tautomer A:

^1H NMR (600 MHz, CDCl_3): δ = 18.23 (s, 1H), 4.98 – 4.95 (m, 1H), 4.75 – 4.71 (m, 1H), 2.70 – 2.66 (m, 1H), 2.57 (s, 3H), 2.50 – 2.47 (m, 1H), 1.95 – 1.82 (m, 4H), 1.62 (s, 3H), 1.53 (s, 3H), 1.48 (s, 3H), 1.43 (s, 3H), 1.28 (s, 3H), 1.26 (s, 3H) ppm.

^{13}C NMR (151 MHz, CDCl_3): δ = 210.3, 201.8, 197.9, 196.6, 140.8, 131.7, 123.9, 117.3, 111.3, 57.1, 56.2, 39.9, 38.7, 27.8, 26.5, 26.2, 25.7, 22.6, 20.6, 17.7, 16.2 ppm.

Tautomer B

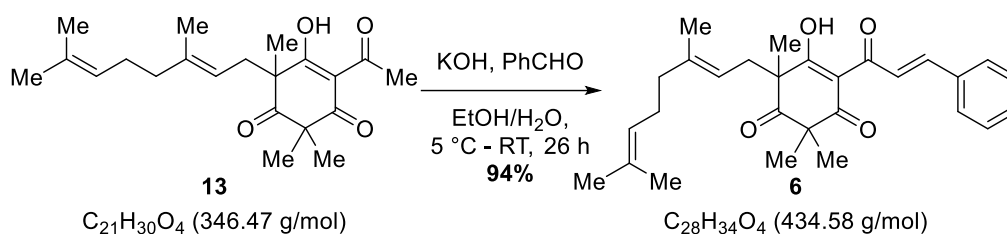
^1H NMR (600 MHz, CDCl_3): δ = 18.19 (s, 1H), 4.98 – 4.95 (m, 1H), 4.79 – 4.76 (m, 1H), 2.59 – 2.55 (m, 1H), 2.57 (s, 3H), 2.42 – 2.39 (m, 1H), 1.95 – 1.82 (m, 4H), 1.62 (s, 3H), 1.53 (s, 3H), 1.51 (s, 3H), 1.40 (s, 3H), 1.38 (s, 3H), 1.30 (s, 3H) ppm.

^{13}C NMR (151 MHz, CDCl_3): δ = 210.0, 201.5, 199.3, 196.5, 139.6, 131.7, 123.9, 118.0, 110.7, 60.9, 52.2, 39.9, 38.2, 27.5, 26.6, 26.4, 25.7, 22.0, 21.2, 17.7, 16.3 ppm.

HRMS (ESI, pos.): m/z calcd for $\text{C}_{21}\text{H}_{31}\text{O}_4^+$ $[\text{M}+\text{H}]^+$: 347.2217, found 347.2216.

IR (ATR): $\tilde{\nu}$ = 2979, 2927, 2874, 1717, 1667, 1555, 1426, 1378, 1360, 1326, 1288, 1234, 1178, 1128, 1108, 1027, 955, 932, 863, 834, 804, 781, 741 cm^{-1} .

8.1.3 4-Cinnamoyl-6-(3,7-dimethylocta-2,6-dien-1-yl)-5-hydroxy-2,2,6-trimethylcyclohex-4-ene-1,3-dione (**6**)



In a round-bottom flask, geranylated acetyl phloroglucinol **13** (17.8 g, 51.4 mmol, 1.0 equiv.) and freshly distilled benzaldehyde (20.8 mL, 21.8 g, 206 mmol, 4.0 equiv.) were dissolved in EtOH (175 mL). The mixture was cooled down to 5 °C using an ice/water-bath and a solution of KOH (7 M, 176 mL) mixed with EtOH (75 mL) was added dropwise through a dropping funnel. After complete addition, the mixture was allowed to warm up to RT and stirred for 18 h. Afterwards, more benzaldehyde (10.4 mL, 10.9 g, 103 mmol, 2.0 equiv.) was added and stirring was continued. After 8 h, crude ^1H -NMR indicated complete consumption of the starting material. The mixture was cooled down to 5 °C using an ice/water-bath and a sat. aq. solution of NH_4Cl (500 mL) was added dropwise through the dropping funnel. The mixture was extracted with cyclohexane (3 x 300 mL). The combined organic layers were dried over Na_2SO_4 , filtered and concentrated under reduced pressure. The residue was dried while stirring under high vacuum for 3 h to remove parts of the excess benzaldehyde. The crude product was purified by column chromatography (SiO_2 , EtOAc:pentane/1:9). After purification, remaining traces of benzaldehyde were removed by stirring under high vacuum at 40 °C over night to afford cinnamoyl phloroglucinol **6** (20.9 g, 48.2 mmol, 94%) as an orange, viscous oil.

The product was isolated as a mixture of two interconverting tautomers (tautomer A : tautomer B = 1:0.8) which gave two sets of signals in the ^1H - and ^{13}C -NMR.

Tautomer A:

^1H NMR (600 MHz, CDCl_3): δ = 18.38 (s, 1H), 8.05 – 7.97 (m, 2H), 7.67 – 7.65 (m, 2H), 7.42 – 7.39 (m, 3H), 5.00 – 4.95 (m, 1H), 4.83 – 4.79 (m, 1H), 2.70 – 2.67 (m, 1H), 2.53 – 2.49 (m,

1H), 1.96 – 1.90 (m, 2H), 1.88 – 1.84 (m, 2H), 1.62 (s, 3H), 1.53 (s, 3H), 1.51 (s, 3H), 1.46 (s, 3H), 1.35 (s, 3H), 1.34 (s, 3H) ppm.

¹³C NMR (151 MHz, CDCl₃): δ = 210.2, 201.8, 197.3, 186.3, 146.7, 140.8, 134.9, 131.7, 131.3, 129.2, 129.1, 124.0, 121.5, 117.3, 110.1, 57.9, 57.8, 39.9, 39.0, 26.6, 26.5, 25.7, 21.9, 20.7, 17.7, 16.3 ppm.

Tautomer B:

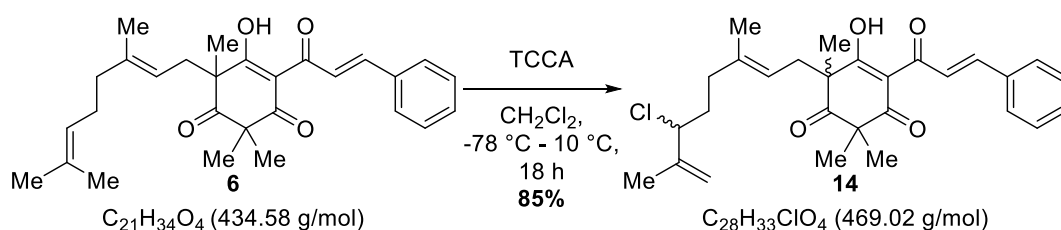
¹H NMR (600 MHz, CDCl₃): δ = 18.11 (s, 1H), 8.05 – 7.97 (m, 2H), 7.67 – 7.65 (m, 2H), 7.42 – 7.39 (m, 3H), 5.00 – 4.95 (m, 1H), 4.88 – 4.85 (m, 1H), 2.65 – 2.61 (m, 1H), 2.46 – 2.42 (m, 1H), 1.96 – 1.90 (m, 2H), 1.88 – 1.84 (m, 2H), 1.63 (s, 3H), 1.51 (s, 6H), 1.44 (s, 3H), 1.40 (s, 3H), 1.38 (s, 3H) ppm.

¹³C NMR (151 MHz, CDCl₃): δ = 209.8, 202.7, 197.4, 185.7, 146.7, 139.8, 134.9, 131.7, 131.3, 129.2, 129.1, 124.0, 121.2, 117.8, 109.8, 61.4, 54.1, 39.9, 38.5, 26.6, 26.2, 25.7, 21.3, 21.0, 17.7, 16.4 ppm.

HRMS (ESI, pos.): *m/z* calcd for C₂₈H₃₄NaO₄⁺ [M+Na]⁺: 457.2349, found 457.2344.

IR (ATR): $\tilde{\nu}$ = 3101, 3058, 2979, 2920, 2878, 2857, 1717, 1665, 1620, 1577, 1518, 1448, 1412, 1378, 1326, 1268, 1209, 1180, 1157, 1108, 1069, 1027, 979, 959, 945, 873, 851, 836, 793, 752 cm⁻¹.

8.1.4 2-(6-Chloro-3,7-dimethylocta-2,7-dien-1-yl)-4-cinnamoyl-5-hydroxy-2,6,6-trimethylcyclohex-4-ene-1,3-dione (**14**)



Gram-scale:

In a Schlenk flask geranylated cinnamoyl phloroglucinol **6** (20.9 g, 48.1 mmol, 1.0 equiv.) was dissolved in CH₂Cl₂ (500 mL) and the mixture was cooled down to -78 °C using a dry ice/isopropanol bath. Then, trichloroisocyanuric acid (TCCA, 5.15 g, 22.2 mmol, 0.46 equiv.) was added and the mixture was allowed to warm up to 10 °C over 18 h. Afterwards, the mixture was diluted with pentane (500 mL) and filtered through a plug of silica. The silica was thoroughly rinsed with EtOAc:pentane/1:9. The filtrate was concentrated under reduced

pressure and the crude product was purified by column chromatography (SiO₂, Et₂O:pentane/1:19) to afford allylic chloride **14** (11.2 g, 23.9 mmol, 50%) as a yellow oil.

Milligram-scale:

According to the above described procedure geranylated cinnamoyl phloroglucinol **6** (98.0 mg, 226 μmol, 1.0 equiv.) was reacted with trichloroisocyanuric acid (24.1 mg, 104 μmol, 0.46 equiv.) in CH₂Cl₂ (2.3 mL). The mixture was diluted with pentane and filtered through a plug of silica which was rinsed with EtOAc:pentane/1:9 until all of the yellow colour was washed out of the silica to afford the pure allylic chloride **14** (90.0 mg, 192 μmol, 85%) as a yellow oil.

The product was isolated as a mixture of two diastereomers which were also interconverting tautomers. Therefore, there are four sets of signals in the ¹H- and ¹³C-NMR. As a result of this, many signals are overlapping which makes a distinguishment between the different sets very complicated. The signals are given without assignment.

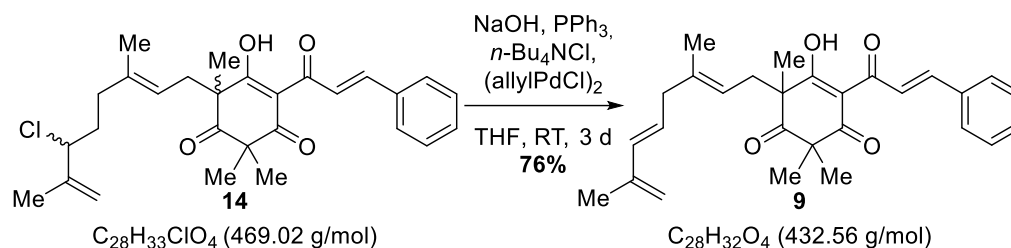
¹H NMR (600 MHz, CDCl₃): δ = 18.34 – 18.11 (m, 1H), 8.04 – 7.99 (m, 2H), 7.67 – 7.65 (m, 2H), 7.43 – 7.41 (m, 3H), 4.96 – 4.93 (m, 1H), 4.92 – 4.83 (m, 1H), 4.83 – 4.79 (m, 1H), 4.25 – 4.20 (m, 1H), 2.71 – 2.60 (m, 1H), 2.54 – 2.42 (m, 1H), 2.01 – 1.95 (m, 1H), 1.91 – 1.85 (m, 1H), 1.84 – 1.75 (m, 2H), 1.74 – 1.71 (m, 3H), 1.52 (s, 3H), 1.47 – 1.44 (m, 3H), 1.41 – 1.38 (m, 3H), 1.36 – 1.34 (m, 3H) ppm.

¹³C NMR (176 MHz, CDCl₃): δ = 210.1, 210.1, 209.7, 209.7, 202.7, 201.8, 201.8, 197.3, 197.2, 197.2, 197.1, 186.3, 186.2, 185.8, 185.8, 146.9, 146.9, 146.9, 144.3, 144.3, 144.3, 139.3, 139.3, 138.2, 134.8, 134.8, 131.4, 131.3, 129.3, 129.2, 129.2, 129.2, 129.2, 129.2, 129.1, 129.1, 121.4, 121.4, 121.1, 121.1, 119.1, 119.0, 118.6, 118.6, 114.4, 114.3, 114.3, 110.1, 109.6, 109.6, 66.2, 66.2, 66.1, 57.9, 57.8, 57.8, 54.1, 54.1, 38.7, 38.7, 38.0, 38.0, 37.0, 36.9, 36.9, 34.7, 34.7, 34.6, 26.5, 26.5, 26.3, 26.3, 22.2, 22.1, 21.5, 21.5, 21.2, 21.2, 20.7, 17.1, 17.0, 16.3, 16.2 ppm.

HRMS (ESI, pos.): *m/z* calcd for C₂₈H₃₃ClNaO₄⁺ [M+Na]⁺: 491.1959, found 491.1966.

IR (ATR): $\tilde{\nu}$ = 3101, 3058, 2979, 2920, 2878, 2857, 1717, 1665, 1620, 1577, 1518, 1448, 1412, 1378, 1326, 1268, 1209, 1180, 1157, 1108, 1069, 1027, 979, 959, 945, 873, 851, 836, 793, 752 cm⁻¹.

8.1.5 4-Cinnamoyl-2-(3,7-dimethylocta-2,5,7-trien-1-yl)-5-hydroxy-2,6,6-trimethylcyclohex-4-ene-1,3-dione (**9**)



A Schlenk flask was loaded with freshly ground NaOH (2.34 g, 58.6 mmol, 2.5 equiv.), PPh₃ (308 mg, 1.17 mmol, 5 mol%) and allylpalladium chloride dimer (85.8 mg, 235 μmol, 1 mol%). The Schlenk-flask was evacuated and backfilled with argon three times. Afterwards, THF (40 mL) and a solution of tetrabutylammonium chloride (40 mM, 16.8 mL, 704 μmol, 3 mol%) were added subsequently. The mixture was stirred vigorously and a solution of allylic chloride **14** (11.0 g, 23.5 mmol, 1.0 equiv.) in THF (50 mL) was added slowly while keeping the mixture at 20 °C using a water bath. Then, the mixture was stirred at RT for 3 d. Afterwards, water (100 mL) was added and the mixture was extracted with EtOAc (3 x 100 mL). The combined organic layers were washed with water, brine, dried over Na₂SO₄, filtered and concentrated under reduced pressure. The crude product was purified by column chromatography (SiO₂, EtOAc:cyclohexane/1:9) to afford diene **9** (7.74 g, 17.8 mmol, 76%) as a yellow oil.

The product was isolated as a mixture of two interconverting tautomers (tautomer A : tautomer B = 1:0.75) which gave two sets of signals in the ¹H- and ¹³C-NMR.

Tautomer A:

¹H NMR (600 MHz, CDCl₃): δ = 18.42 (s, 1H), 8.04–7.98 (m, 2H), 7.67–7.65 (m, 2H), 7.43–7.40 (m, 3H), 6.05–6.00 (m, 1H), 5.46–5.40 (m, 1H), 4.90–4.80 (m, 3H), 2.73–2.66 (m, 1H), 2.64–2.61 (m, 2H), 2.54–2.44 (m, 1H), 1.75 (s, 3H), 1.51 (s, 3H), 1.48 (s, 3H), 1.35 (s, 3H), 1.33 (s, 3H) ppm.

¹³C NMR (151 MHz, CDCl₃): δ = 210.3, 201.7, 197.2, 186.4, 146.8, 142.0, 139.7, 134.9, 134.8, 131.3, 129.2, 129.1, 127.7, 121.5, 118.3, 115.0, 110.3, 58.0, 57.6, 43.0, 39.2, 26.4, 22.3, 20.3, 18.7, 16.5 ppm.

Tautomer B:

¹H NMR (600 MHz, CDCl₃): δ = 18.12 (s, 1H), 8.04 – 7.98 (m, 2H), 7.67 – 7.65 (m, 2H), 7.43 – 7.40 (m, 3H), 6.05 – 6.00 (m, 1H), 5.46 – 5.40 (m, 1H), 4.90 – 4.80 (m, 3H), 2.73 – 2.66 (m, 1H), 2.64 – 2.61 (m, 2H), 2.54 – 2.44 (m, 1H), 1.74 (s, 3H), 1.51 (s, 3H), 1.42 (s, 3H), 1.40 (s, 6H) ppm.

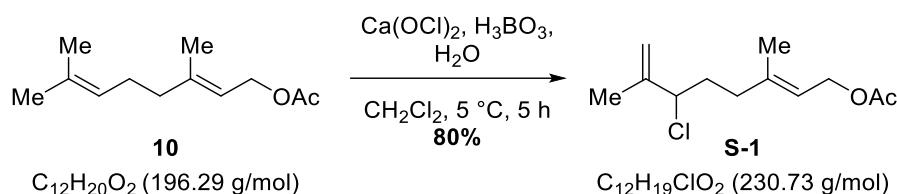
¹³C NMR (151 MHz, CDCl₃): δ = 210.0, 202.7, 197.4, 185.7, 146.8, 141.9, 138.6, 134.9, 134.8, 131.3, 129.2, 129.2, 127.6, 121.2, 118.9, 115.1, 109.9, 61.1, 54.3, 43.0, 38.6, 26.6, 21.6, 21.1, 18.7, 16.6 ppm.

HRMS (ESI, pos.): *m/z* calcd for C₂₈H₃₂NaO₄⁺ [M+Na]⁺: 455.2193, found 455.2201.

IR (ATR): $\tilde{\nu}$ = 3101, 3082, 3024, 2980, 2931, 2871, 2853, 1717, 1666, 1620, 1577, 1519, 1449, 1415, 1380, 1327, 1305, 1266, 1209, 1181, 1158, 1118, 1026, 966, 946, 884, 854, 839, 794, 752 cm⁻¹.

8.2 Convergent Route to Intermediate 9

8.2.1 6-Chloro-3,7-dimethylocta-2,7-dien-1-yl acetate (**S-1**)



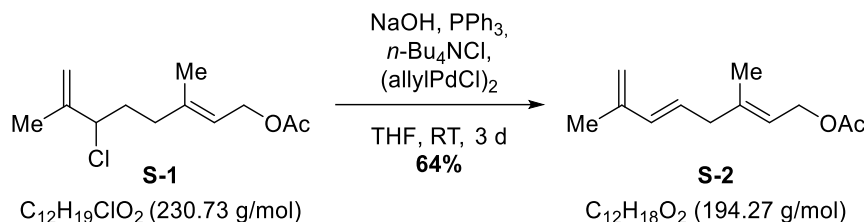
Calcium hypochlorite (67 w%, 6.47 g, 30.6 mmol, 0.6 equiv.) and boric acid (7.58 g, 122 mmol, 2.4 equiv.) were suspended in CH₂Cl₂ (50 mL) in an Erlenmeyer flask. The resulting mixture was cooled down to 5 °C using an ice-water bath and geranyl acetate (**10**) (11.0 mL, 10.0 g, 50.9 mmol, 1.0 equiv.) was added. Under vigorous stirring, water (13.8 mL) was added over 5 h. After complete conversion of the starting material, solid Na₂SO₃ was added, the inorganic salts were filtered off through a plug of celite and the filtrate was concentrated under reduced pressure. The crude product was purified by column chromatography (SiO₂, EtOAc/pentane, 1:19 to 1:9) to afford allylic chloride **S-1** (9.37 g, 40.6 mmol, 80%) as a colorless oil.

¹H NMR (600 MHz, CDCl₃): δ = 5.37 (tq, *J* = 7.0, 1.3 Hz, 1H), 5.01 – 5.00 (m, 1H), 4.90 (p, *J* = 1.5 Hz, 1H), 4.58 (d, *J* = 7.1 Hz, 2H), 4.35 – 4.32 (m, 1H), 2.19 – 2.13 (m, 2H), 2.05 (s, 3H), 2.01 – 1.88 (m, 2H), 1.81 (s, 3H), 1.71 (s, 3H) ppm.

¹³C NMR (151 MHz, CDCl₃): δ = 171.2, 144.3, 140.7, 119.5, 114.5, 66.3, 61.3, 36.6, 34.5, 21.2, 17.1, 16.6 ppm.

The spectroscopic data are in accordance with the literature.⁸

8.2.2 3,7-Dimethylocta-2,5,7-trien-1-yl acetate (**S-2**)



The dehydrochlorination of allylic chloride **S-1** was performed according to a literature known procedure.⁹ Freshly ground NaOH (3.57 g, 89.2 mmol, 1.1 equiv.), PPh₃ (1.06 g, 4.05 mmol, 5 mol%) and *n*-Bu₄NCl (676 mg, 2.43 mmol, 3 mol%) were loaded into a Schlenk flask. The flask was evacuated and backfilled with argon three times. Afterwards, THF (60 mL) and allylic chloride **S-1** (18.7 g, 81.0 mmol, 1.0 equiv.) dissolved in THF (100 mL) were added to the mixture subsequently while keeping the temperature under 25 °C. The mixture was stirred for three days. Afterwards, water (100 mL) was added, the phases were separated and the aqueous phase was extracted with diethyl ether (3 x 100 mL). The combined organic phases were washed with water, brine, dried over Na₂SO₄, filtered and concentrated under reduced pressure. The crude product was purified by column chromatography (SiO₂, EtOAc/pentane, 1:19) to afford diene **S-2** (10.0 g, 51.5 mmol, 64%) as a yellowish oil.

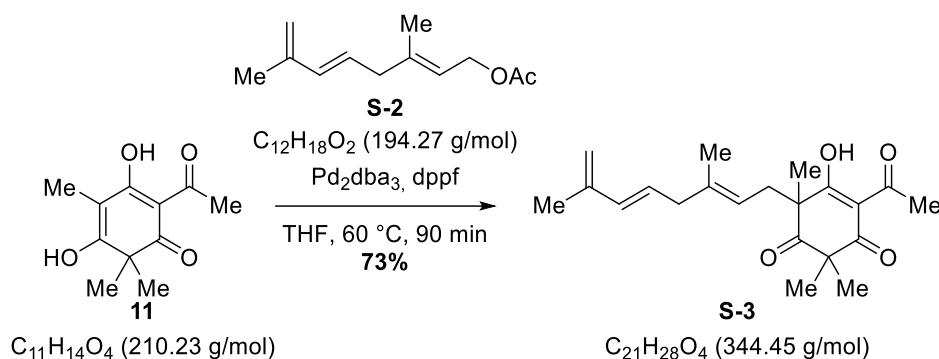
¹H NMR (600 MHz, CDCl₃): δ = 6.16 (d, *J* = 15.6 Hz, 1H), 5.61 (dt, *J* = 15.5, 7.1 Hz, 1H), 5.37 (tq, *J* = 7.1, 1.4 Hz, 1H), 4.91 – 4.90 (m, 2H), 4.60 (d, *J* = 7.3 Hz, 2H), 2.82 (d, *J* = 7.1 Hz, 2H), 2.06 (s, 3H), 1.84 (s, 3H), 1.70 (s, 3H) ppm.

¹³C NMR (151 MHz, CDCl₃): δ = 171.3, 142.0, 141.2, 135.0, 127.5, 119.3, 115.3, 61.5, 42.8, 21.2, 18.8, 16.8 ppm.

HRMS (ESI, pos.): *m/z* calcd for C₁₂H₁₈O₂Na⁺ [M+Na]⁺: 217.1199, found 217.1193.

IR (ATR): $\tilde{\nu}$ = 3081, 3022, 2975, 2942, 2919, 1737, 1672, 1649, 1608, 1438, 1380, 1365, 1319, 1227, 1109, 1021, 966, 884, 826, 793, 777, 747, 719 cm⁻¹.

8.2.3 4-Acetyl-6-(3,7-dimethylocta-2,5,7-trien-1-yl)-5-hydroxy-2,2,6-trimethylcyclohex-4-ene-1,3-dione (**S-3**)



A Schlenk flask was loaded with trimethylated acetyl-phloroglucinol **11** (5.80 g, 27.6 mmol, 1.0 equiv.), $\text{Pd}_2(\text{dba})_3$ (632 mg, 690 μmol , 2.5 mol%) and dppf (765 mg, 1.38 mmol, 5 mol%). The flask was evacuated and backfilled with argon three times. Afterwards, dry THF (200 mL) and allylic acetate **S-2** (8.04 g, 41.4 mmol, 1.5 equiv.) were added subsequently and the mixture was heated to 60 $^\circ\text{C}$. After stirring at this temperature for 90 min, the mixture was allowed to cool down to RT and filtered through a plug of silica. The silica was thoroughly rinsed with EtOAc. The filtrate was concentrated under reduced pressure and the crude product was purified by column chromatography (SiO_2 , Et_2O /pentane, 1:19 to 1:9) to afford diene **S-3** (6.90 g, 20.0 mmol, 73%) as a yellowish oil.

The product was isolated as a mixture of two interconverting tautomers (tautomer A : tautomer B = 1:0.7) which gave two sets of signals in the ^1H - and ^{13}C -NMR.

Tautomer A:

^1H NMR (600 MHz, CD_2Cl_2): δ = 18.23 (s, 1H), 6.08 – 6.04 (m, 1H), 5.51 – 5.43 (m, 1H), 4.88 – 4.78 (m, 3H), 2.73 – 2.58 (m, 3H), 2.56 (s, 3H), 2.53 – 2.41 (m, 1H), 1.80 (s, 3H), 1.50 (s, 3H), 1.45 (s, 3H), 1.29 (s, 3H), 1.24 (s, 3H) ppm.

^{13}C NMR (151 MHz, CD_2Cl_2): δ = 210.5, 202.2, 197.9, 196.6, 142.5, 139.8, 134.9, 128.1, 118.7, 115.0, 111.7, 57.6, 56.3, 43.2, 39.0, 27.8, 26.4, 23.0, 20.4, 18.8, 16.5 ppm.

Tautomer B

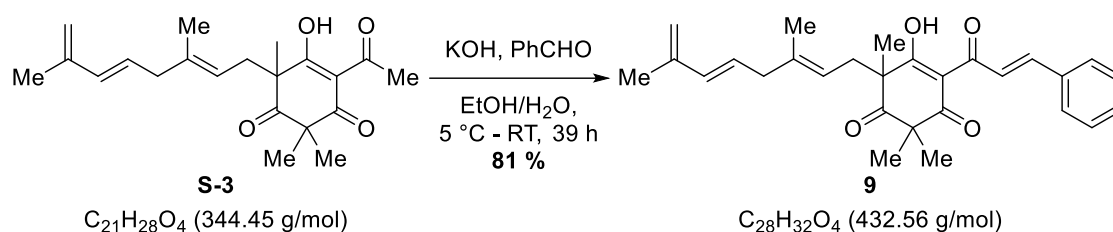
^1H NMR (600 MHz, CD_2Cl_2): δ = 18.20 (s, 1H), 6.08 – 6.04 (m, 1H), 5.51 – 5.43 (m, 1H), 4.88 – 4.78 (m, 3H), 2.73 – 2.58 (m, 3H), 2.56 (s, 3H), 2.53 – 2.41 (m, 1H), 1.79 (s, 3H), 1.53 (s, 3H), 1.39 (s, 6H), 1.31 (s, 3H) ppm.

^{13}C NMR (151 MHz, CD_2Cl_2): δ = 210.2, 201.7, 199.6, 196.5, 142.4, 138.6, 134.9, 128.2, 119.4, 115.1, 111.1, 60.9, 52.5, 43.2, 38.4, 27.6, 26.6, 22.0, 21.6, 18.8, 16.5 ppm.

HRMS (ESI, pos.): m/z calcd for $\text{C}_{21}\text{H}_{28}\text{NaO}_4^+$ $[\text{M}+\text{Na}]^+$: 367.1880, found 367.1896.

IR (ATR): $\tilde{\nu}$ = 3082, 2976, 2936, 2874, 2853, 1739, 1718, 1670, 1607, 1556, 1453, 1434, 1381, 1364, 1323, 1229, 1177, 1124, 1025, 966, 928, 882, 861, 836, 794, 779, 743, 722 cm^{-1} .

8.2.4 4-Cinnamoyl-6-(3,7-dimethylocta-2,5,7-trien-1-yl)-5-hydroxy-2,2,6-trimethylcyclohex-4-ene-1,3-dione (**9**)



In a round-bottom flask, a mixture of aq. KOH (7 M, 15 mL, 24 equiv.) and EtOH (15 mL) was cooled down to 5 °C using an ice-water bath. Acetyl phloroglucinol **S-3** (1.70 g, 4.94 mmol, 1.0 equiv.) and benzaldehyde (1.00 mL, 1.05 g, 9.87 mmol, 2.0 equiv.) dissolved in EtOH (15 mL) were added slowly. Then, the mixture was allowed to warm up to RT. After stirring the mixture at this temperature for 16 h, more benzaldehyde (1.00 mL, 1.05 g, 9.87 mmol, 2 equiv.) was added. Stirring was continued for 7 h. Then, more benzaldehyde (1.00 mL, 1.05 g, 9.87 mmol, 2 equiv.) was added. After another 16 h the starting material was consumed completely. The mixture was poured into an ice-cold sat. aq. solution of ammonium chloride (100 mL) and extracted with EtOAc (3 x 100 mL). The combined organic layers were washed with water, brine, dried over Na_2SO_4 , filtered and concentrated under reduced pressure. The residue was dried while stirring under high vacuum for 3 h to remove parts of the excess benzaldehyde. The crude product was purified by column chromatography (SiO_2 , Et_2O /pentane, 1:19). After purification, the product was once more dried while stirring under high vacuum over night to remove the remaining traces of benzaldehyde to afford cinnamoyl phloroglucinol **9** (1.73 g, 4.00 mmol, 81%) as a yellow, thick oil.

The product was isolated as a mixture of two interconverting tautomers (tautomer A : tautomer B = 1:0.75) which gave two sets of signals in the ^1H - and ^{13}C -NMR.

Tautomer A:

¹H NMR (600 MHz, CDCl₃): δ = 18.42 (s, 1H), 8.04–7.98 (m, 2H), 7.67–7.65 (m, 2H), 7.43–7.40 (m, 3H), 6.05–6.00 (m, 1H), 5.46–5.40 (m, 1H), 4.90–4.80 (m, 3H), 2.73–2.66 (m, 1H), 2.64–2.61 (m, 2H), 2.54–2.44 (m, 1H), 1.75 (s, 3H), 1.51 (s, 3H), 1.48 (s, 3H), 1.35 (s, 3H), 1.33 (s, 3H) ppm.

¹³C NMR (151 MHz, CDCl₃): δ = 210.3, 201.7, 197.2, 186.4, 146.8, 142.0, 139.7, 134.9, 134.8, 131.3, 129.2, 129.1, 127.7, 121.5, 118.3, 115.0, 110.3, 58.0, 57.6, 43.0, 39.2, 26.4, 22.3, 20.3, 18.7, 16.5 ppm.

Tautomer B:

¹H NMR (600 MHz, CDCl₃): δ = 18.12 (s, 1H), 8.04–7.98 (m, 2H), 7.67–7.65 (m, 2H), 7.43–7.40 (m, 3H), 6.05–6.00 (m, 1H), 5.46–5.40 (m, 1H), 4.90–4.80 (m, 3H), 2.73–2.66 (m, 1H), 2.64–2.61 (m, 2H), 2.54–2.44 (m, 1H), 1.74 (s, 3H), 1.51 (s, 3H), 1.42 (s, 3H), 1.40 (s, 6H) ppm.

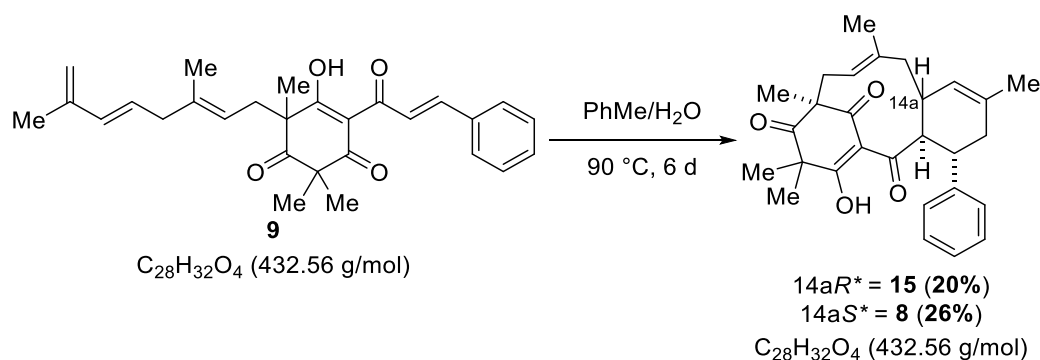
¹³C NMR (151 MHz, CDCl₃): δ = 210.0, 202.7, 197.4, 185.7, 146.8, 141.9, 138.6, 134.9, 134.8, 131.3, 129.2, 129.2, 127.6, 121.2, 118.9, 115.1, 109.9, 61.1, 54.3, 43.0, 38.6, 26.6, 21.6, 21.1, 18.7, 16.6 ppm.

HRMS (ESI, pos.): *m/z* calcd for C₂₈H₃₂NaO₄⁺ [M+Na]⁺: 455.2193, found 455.2201.

IR (ATR): $\tilde{\nu}$ = 3101, 3082, 3024, 2980, 2931, 2871, 2853, 1717, 1666, 1620, 1577, 1519, 1449, 1415, 1380, 1327, 1305, 1266, 1209, 1181, 1158, 1118, 1026, 966, 946, 884, 854, 839, 794, 752 cm⁻¹.

8.3 IMDA and Backbone Oxidation

8.3.1 IMDA-diastereomers **15** and **8**



In a two-necked round-bottom flask equipped with a reflux condenser, diene **9** (7.70 g, 17.8 mmol, 1.0 equiv.) was dissolved in toluene (500 mL). Water (500 mL) was added and the mixture was degassed by bubbling through a stream of argon while stirring vigorously for 5 h.

Afterwards, the mixture was heated to 90 °C for 6 d. After allowing the mixture to cool down to RT, the phases were separated and the aqueous phase was extracted with EtOAc (3 x 100 mL). The combined organic layers were washed with brine, dried over Na₂SO₄, filtered and concentrated under reduced pressure. Pentane was added to the residue and the mixture was filtered. The solids were collected, cyclohexane was added and the suspension was sonicated for 30 min. The mixture was filtered again and the solid was dried in the high vacuum to afford diastereomer **8** (2.00 g, 4.64 mmol, 26%) as a white, amorphous solid. The filtrate of the second filtration was concentrated under reduced pressure, pentane was added and the suspension was sonicated for 10 min. The solid was filtered off and dried in the high vacuum to afford diastereomer **15** (1.55 g, 3.58 mmol, 20%) as a white, amorphous solid.

Analytical data for compound **15**:

¹H NMR (600 MHz, CDCl₃): δ = 17.50 (s, 1H), 7.40–7.39 (m, 2H), 7.19–7.16 (m, 2H), 7.08–7.05 (m, 1H), 5.20–5.18 (m, 1H), 5.00–4.97 (m, 1H), 3.44 (dd, *J* = 11.0, 9.8 Hz, 1H), 3.19 (td, *J* = 11.7, 4.4 Hz, 1H), 3.12–3.06 (m, 1H), 2.41–2.34 (m, 1H), 2.33–2.29 (m, 1H), 2.19 (dd, *J* = 13.8, 12.1 Hz, 1H), 2.14–2.10 (m, 1H), 1.99–1.95 (m, 1H), 1.80 (t, *J* = 12.5 Hz, 1H), 1.72 (s, 3H), 1.40 (s, 3H), 1.34 (s, 3H), 1.33 (s, 3H), 0.98 (s, 3H) ppm.

¹³C NMR (151 MHz, CDCl₃): δ = 206.3, 202.6, 196.4, 195.8, 142.3, 140.5, 133.6, 128.9, 127.9, 126.4, 124.8, 120.1, 114.4, 60.5, 52.0, 49.0, 48.3, 46.0, 42.2, 38.6, 37.1, 28.2, 23.4, 20.0, 16.6, 15.5 ppm.

HRMS (ESI, pos.): *m/z* calcd for C₂₈H₃₂KO₄⁺ [*M*+*K*]⁺: 471.1933, found 471.1914.

IR (ATR): $\tilde{\nu}$ = 3029, 2979, 2913, 2878, 2850, 1722, 1684, 1539, 1495, 1454, 1387, 1376, 1361, 1345, 1310, 1217, 1162, 1141, 1103, 1082, 1025, 950, 923, 907, 897, 881, 840, 818, 800, 753 cm⁻¹.

X-ray: Crystals were grown by the vapor diffusion technique of a solution of **15** in CH₂Cl₂ with *n*-pentane at ambient temperature.

Analytical data for compound **8**:

¹H NMR (600 MHz, CDCl₃): δ = 17.96 (s, 1H), 7.37–7.32 (m, 4H), 7.23–7.21 (m, 1H), 5.18 (brs, 1H), 4.59–4.56 (m, 1H), 3.55–3.54 (m, 1H), 3.38–3.36 (m, 1H), 2.86–2.83 (m, 1H), 2.81–2.76 (m, 1H), 2.38 (t, *J* = 12.7 Hz, 1H), 2.29–2.26 (m, 1H), 2.24–2.18 (m, 2H), 1.89 (s, 3H), 1.78–1.74 (m, 1H), 1.45 (s, 3H), 1.44 (s, 3H), 1.38 (s, 3H), 1.16 (s, 3H) ppm.

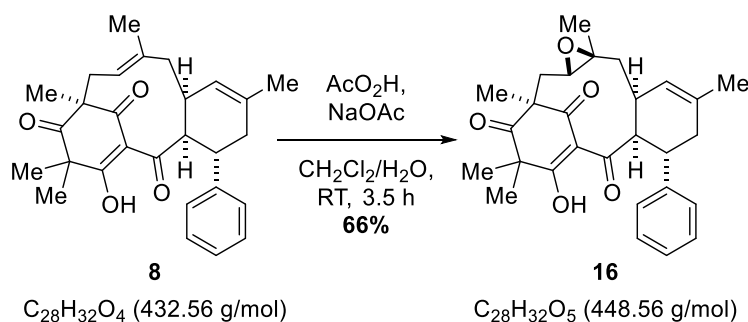
^{13}C NMR (151 MHz, CDCl_3): δ = 209.2, 201.3, 200.7, 194.7, 144.9, 134.8, 134.4, 128.5, 127.3, 126.5, 124.9, 123.4, 117.0, 59.1, 56.0, 43.4, 43.0, 39.5, 39.5, 32.1, 30.8, 28.2, 23.6, 22.9, 16.7, 14.2 ppm.

HRMS (ESI, pos.): m/z calcd for $\text{C}_{28}\text{H}_{32}\text{NaO}_4^+$ $[\text{M}+\text{Na}]^+$: 455.2193, found 455.2181.

IR (ATR): $\tilde{\nu}$ = 3062, 3024, 2979, 2906, 2852, 1722, 1675, 1541, 1495, 1466, 1450, 1370, 1360, 1316, 1296, 1268, 1216, 1180, 1153, 1081, 1068, 1030, 993, 958, 930, 881, 841, 809, 756, 703 cm^{-1} .

X-ray: Crystals were grown by the vapor diffusion technique of a solution of **8** in CH_2Cl_2 with *n*-pentane at ambient temperature.

8.3.2 Epoxide 16



In a round-bottom flask, epoxide **8** (2.00 g, 4.64 mmol, 1.0 equiv.) was dissolved in CH_2Cl_2 (14 mL). 1 M aq. NaOAc (23 mL) was added to the mixture. Under vigorous stirring, acetic acid peroxide (35 w% in acetic acid, 2.95 mL, 3.33 g, 15.3 mmol, 3.33 equiv.) was added over 3.5 h. Afterwards, the mixture was cooled down to 5 °C using an ice/water-bath and sat. aq. $\text{Na}_2\text{S}_2\text{O}_3$ (50 mL) was added slowly under vigorously stirring. Then, the phases were separated and the aqueous phase was extracted with CH_2Cl_2 (3 x 20 mL). The combined organic layers were washed with aq. sat. NaHCO_3 , water, brine, dried over Na_2SO_4 , filtered and concentrated under reduced pressure. The crude product was purified by column chromatography (SiO_2 , CH_2Cl_2) to afford epoxide **16** (1.38 g, 3.08 mmol, 66%) as a white, amorphous solid.

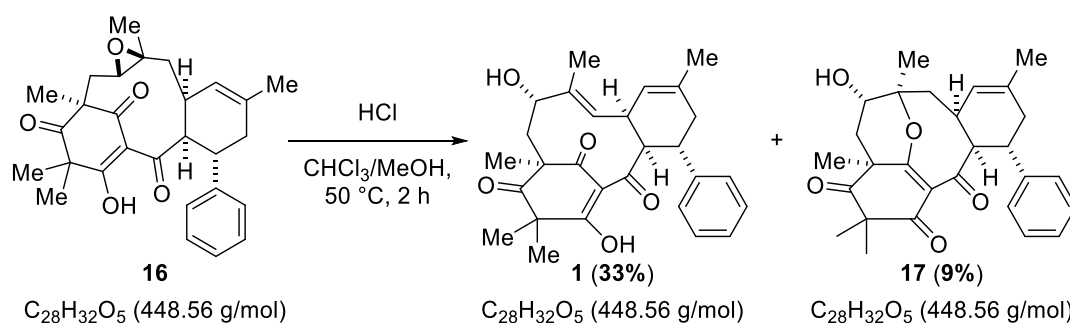
^1H NMR (600 MHz, CD_2Cl_2): δ = 17.95 (s, 1H), 7.40 – 7.39 (m, 2H), 7.36 – 7.34 (m, 2H), 7.25 – 7.23 (m, 1H), 5.14 (s, 1H), 3.95 (d, J = 6.0 Hz, 1H), 3.45 (d, J = 6.6 Hz, 1H), 2.80 – 2.75 (m, 1H), 2.68 (d, J = 13.2 Hz, 1H), 2.30 – 2.27 (m, 1H), 2.21 – 2.19 (m, 1H), 2.14 – 2.10 (m, 1H), 1.97 (dd, J = 13.8, 5.1 Hz, 1H), 1.86 (s, 3H), 1.48 (s, 3H), 1.44 (s, 3H), 1.38 (s, 3H), 1.35 – 1.34 (m, 1H), 0.85 (t, J = 13.8 Hz, 1H), 0.74 (s, 3H) ppm.

^{13}C NMR (151 MHz, CD_2Cl_2): δ = 209.0, 200.0, 199.5, 199.1, 144.9, 134.7, 128.8, 127.5, 126.9, 123.4, 115.5, 64.3, 60.0, 58.6, 57.0, 42.7, 40.7, 39.7, 37.8, 33.2, 30.9, 28.1, 23.5, 23.2, 16.7, 16.1 ppm.

HRMS (ESI, neg.): m/z calcd for $\text{C}_{28}\text{H}_{31}\text{O}_5^-$ [M-H] $^-$: 447.2177, found 447.2169.

IR (ATR): $\tilde{\nu}$ = 3024, 2976, 2908, 2861, 1724, 1672, 1542, 1495, 1450, 1427, 1386, 1370, 1318, 1297, 1280, 1254, 1218, 1183, 1166, 1117, 1065, 1050, 1028, 990, 978, 967, 945, 926, 883, 865, 813, 753, 702 cm^{-1} .

8.3.3 (\pm)-Cleistocaltone A (**1**)



In a two-necked round-bottom flask equipped with a dropping funnel, epoxide **16** (1.74 g, 4.02 mmol, 1.0 equiv.) was dissolved in CHCl_3 (150 mL). The flask was capped and the mixture was heated to 50 °C. HCl (1 w% in MeOH, 92.9 mL, 20.1 mmol, 5.0 equiv.) was added through the dropping funnel and the mixture was stirred for 2 h. Afterwards, the mixture was concentrated under reduced pressure. The crude product was purified by flash column chromatography (SiO_2 , EtOAc/pentane, 1:4) to afford (\pm)-Cleistocaltone A (**1**) (587 mg, 1.30 mmol, 33%) as a white amorphous solid and side product **17** (162 mg, 361 μmol , 9%) as a white amorphous solid.

Analytical data of (\pm)-Cleistocaltone A (**1**):

^1H NMR (700 MHz, CDCl_3): δ = 16.46 (s, 1H), 7.33 – 7.31 (m, 2H), 7.24 – 7.22 (m, 1H), 7.21 – 7.20 (m, 2H), 5.09 – 5.08 (m, 1H), 4.85 (dd, J = 9.9, 1.6 Hz, 1H), 4.22 – 4.21 (m, 1H), 3.75 (dd, J = 11.4, 2.6 Hz, 1H), 3.48 – 3.46 (m, 1H), 3.05 – 3.02 (m, 2H), 2.50 (dd, J = 13.2, 2.8 Hz, 1H), 2.21 – 2.18 (m, 1H), 2.13 (dd, J = 13.2, 11.5 Hz, 1H), 1.81 (s, 3H), 1.50 (s, 3H), 1.47 (s, 3H), 1.32 (s, 3H), 1.18 (d, J = 1.4 Hz, 3H) ppm.

^{13}C NMR (151 MHz, CDCl_3): δ = 210.9, 207.1, 196.4, 187.3, 146.0, 138.2, 136.2, 131.5, 128.6, 127.4, 126.5, 120.3, 116.3, 75.0, 56.7, 51.0, 47.9, 45.2, 38.1, 32.3, 32.0, 28.8, 27.5, 23.7, 20.1, 8.9 ppm.

HRMS (ESI, pos.): m/z calcd for $C_{28}H_{32}NaO_5^+$ $[M+Na]^+$: 471.2142, found 471.2147.

IR (ATR): $\tilde{\nu}$ = 3474, 3394, 2924, 2851, 1716, 1659, 1568, 1495, 1451, 1402, 1378, 1243, 1102, 1031, 956, 864, 767, 737 cm^{-1} .

The spectroscopic data are in accordance with the literature.¹⁰

Analytical data of sideproduct **17**:

1H NMR (700 MHz, $CDCl_3$) δ = 7.30 – 7.28 (m, 2H), 7.22 – 7.20 (m, 1H), 7.16 – 7.15 (m, 2H), 5.04 (brs, 1H), 3.85 (brs, 1H), 3.59 (dd, J = 4.3, 2.2 Hz, 1H), 3.54 (dd, J = 5.4, 3.7 Hz, 1H), 2.72 – 2.68 (m, 1H), 2.46 – 2.44 (m, 1H), 2.34 (dd, J = 15.0, 2.2 Hz, 1H), 2.15 – 2.09 (m, 3H), 2.05 – 2.01 (m, 1H), 1.71 (s, 3H), 1.70 (s, 3H), 1.45 (s, 3H), 1.38 (dd, J = 15.1, 6.1 Hz, 1H), 1.27 (s, 3H), 1.25 (s, 3H) ppm.

^{13}C NMR (176 MHz, $CDCl_3$) δ = 210.6, 198.1, 195.0, 175.6, 145.5, 135.6, 128.5, 127.6, 127.4, 126.3, 123.7, 89.7, 70.5, 59.1, 56.1, 46.6, 39.0, 37.9, 36.7, 31.9, 27.7, 27.2, 23.9, 23.3, 19.2, 19.1 ppm.

HRMS (ESI, pos.): m/z calcd for $C_{28}H_{32}NaO_5^+$ $[M+Na]^+$: 471.2142, found 471.2157.

IR (ATR): $\tilde{\nu}$ = 3467, 2982, 2961, 2924, 2855, 1718, 1689, 1645, 1622, 1495, 1453, 1381, 1353, 1320, 1246, 1220, 1178, 1145, 1092, 1050, 1010, 992, 971, 940, 921, 902, 852, 822, 795, 754, 712, 702 cm^{-1} .

X-ray: Crystals were grown by slow evaporation of a solution of **17** in diethyl ether at ambient temperature. The compound crystallized with one diethyl ether molecule in the cell.

9. Comparison of NMR Data

9.1 (±)-Cleistocaltone A (1)

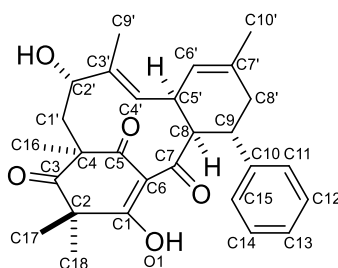


Table 1. Comparison of ^1H and ^{13}C NMR Data for Isolated and Synthetic (±)-Cleistocaltone A (1).^a

No.	Isolation ^b ^{13}C NMR (125 MHz) $\delta_{\text{C}}/\text{ppm}^{\text{c}}$	Synthetic ^{13}C NMR (176 MHz) $\delta_{\text{C}}/\text{ppm}^{\text{c}}$	Δ/ppm	Isolation ^b ^1H NMR (500 MHz) $\delta_{\text{H}}/\text{ppm}$ (J in Hz) ^d	Synthetic ^1H NMR (700 MHz) $\delta_{\text{H}}/\text{ppm}$ (J in Hz) ^c	Δ/ppm
1	187.1	187.3	0.2			
2	50.9	51.0	0.1			
3	210.9	210.9	0.0			
4	56.6	56.7	0.1			
5	196.2	196.4	0.2			
6	116.2	116.3	0.1			
7	206.9	207.1	0.2			
8	38.0	38.1	0.1	3.53 m	3.47 m	0.06
9	47.9	47.9	0.0	4.27 m	4.21 m	0.06
10	145.9	146.0	0.1			
11	127.2	127.4	0.2	7.28 m	7.20 m	0.08
12	128.5	128.6	0.1	7.37	7.32	0.05
13	126.4	126.5	0.1	7.28	7.23	0.05
14	128.5	128.6	0.1	7.37	7.32	0.05
15	127.3	127.4	0.1	7.28 m	7.20 m	0.08
16	27.4	27.5	0.1	1.37 s	1.32 s	0.05
17	28.6	28.8	0.2	1.56 s	1.50 s	0.06
18	20.0	20.1	0.1	1.52 s	1.47 s	0.05
1'a	45.2	45.2	0.0	2.54 dd (13.2, 2.7)	2.50 dd (13.2, 2.8)	0.04
1'b				2.16 dd (13.2, 11.3)	2.13 dd (13.2, 11.5)	0.03
2'	74.8	75.0	0.2	3.80 dd (11.3, 2.7)	3.75 dd (11.4, 2.6)	0.05
3'	138.3	138.2	0.1			
4'	131.2	131.5	0.3	4.90 d (9.9)	4.85 dd (9.9, 1.6)	0.05
5'	31.9	32.0	0.1	3.10	3.04	0.06
6'	120.3	120.3	0.0	5.15 m	5.09 m	0.06
7'	136.0	136.2	0.2			
8'a	32.2	32.3	0.1	3.10	3.04	0.06
8'b				2.26 m	2.20 m	0.06
9'	8.8	8.9	0.1	1.23 s	1.18 d (1.4)	0.05
10'	23.5	23.7	0.2	1.87 s	1.81 s	0.06
1-OH				16.51 s	16.46 s	0.05

a) All data were obtained in CDCl_3 . Overlapped signals were reported without designating multiplicity. b) Data from reference 6. c) Chemical shifts are reported relative to the corresponding residual non-deuterated solvent signal (CDCl_3 : $\delta_{\text{H}} = 7.26$ ppm, $\delta_{\text{C}} = 77.16$ ppm). d) Chemical shifts are reported relative to TMS ($\delta_{\text{H}} = 0.00$ ppm).

10. X-ray data

10.1 IMDA-diastereomer 15

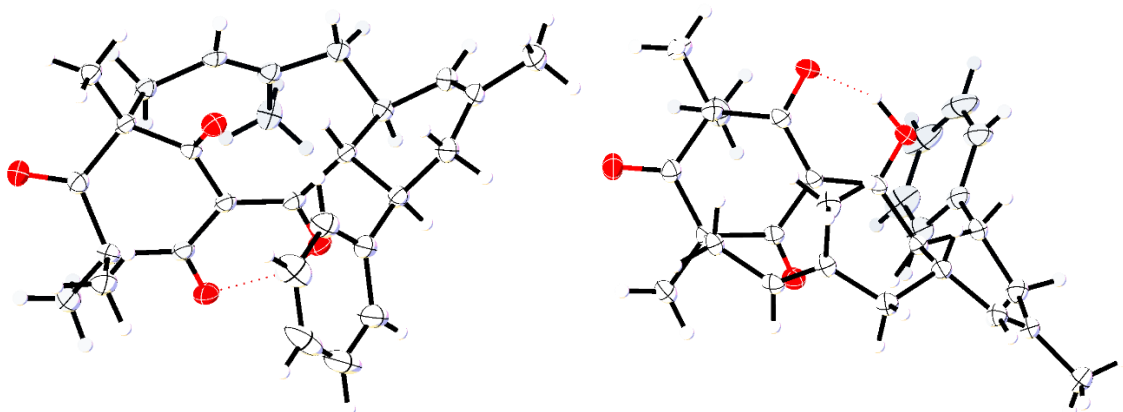


Table 2. Crystal data of IMDA-diastereomer 15

Empirical formula	C ₂₈ H ₃₂ O ₄
Formula weight	432.53
Temperature/K	140(2)
Crystal system	monoclinic
Space group	P2 ₁ /n
a/Å	9.53542(6)
b/Å	18.20996(12)
c/Å	14.54563(9)
α/°	90
β/°	105.5556(2)
γ/°	90
Volume/Å ³	2433.18(3)
Z	4
ρ _{calc} /cm ³	1.181
μ/mm ⁻¹	0.617
F(000)	928.0
Crystal size/mm ³	0.44 × 0.25 × 0.14
Radiation	CuKα (λ = 1.54178)
2θ range for data collection/°	7.96 to 144.238
Index ranges	-11 ≤ h ≤ 11, -22 ≤ k ≤ 22, -14 ≤ l ≤ 17
Reflections collected	33228
Independent reflections	4766 [R _{int} = 0.0376, R _{sigma} = 0.0210]
Data/restraints/parameters	4766/0/296
Goodness-of-fit on F ²	1.049
Final R indexes [I ≥ 2σ (I)]	R ₁ = 0.0392, wR ₂ = 0.0938
Final R indexes [all data]	R ₁ = 0.0402, wR ₂ = 0.0943
Largest diff. peak/hole / e Å ⁻³	0.22/-0.30

10.2 IMDA-diastereomer 8

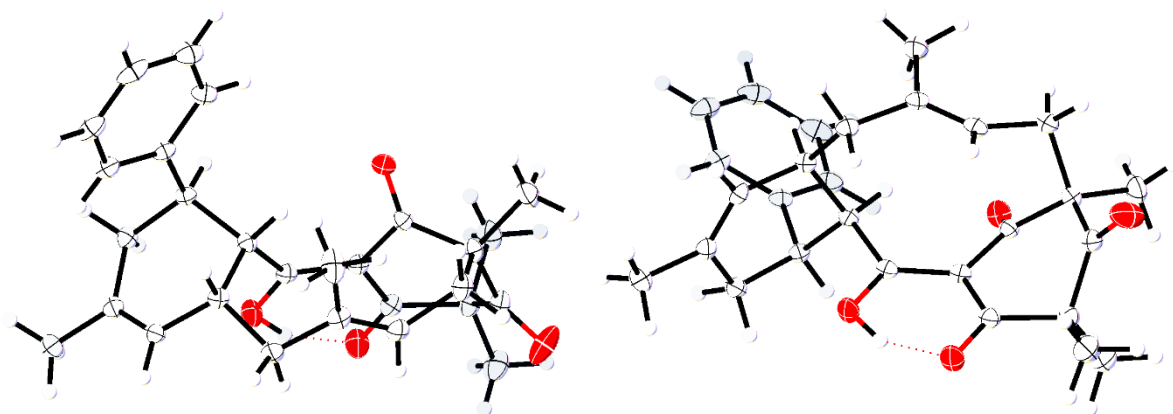


Table 3. Crystal data of IMDA-diastereomer 8

Empirical formula	C ₂₈ H ₃₂ O ₄
Formula weight	432.53
Temperature/K	140(2)
Crystal system	monoclinic
Space group	P2 ₁ /n
a/Å	8.38079(5)
b/Å	23.63124(15)
c/Å	12.06328(8)
α/°	90
β/°	106.2413(2)
γ/°	90
Volume/Å ³	2293.77(3)
Z	4
ρ _{calc} /cm ³	1.253
μ/mm ⁻¹	0.655
F(000)	928.0
Crystal size/mm ³	0.39 × 0.23 × 0.1
Radiation	CuKα (λ = 1.54178)
2Θ range for data collection/°	7.482 to 144.09
Index ranges	-10 ≤ h ≤ 9, -28 ≤ k ≤ 29, -14 ≤ l ≤ 14
Reflections collected	34216
Independent reflections	4516 [R _{int} = 0.0478, R _{sigma} = 0.0240]
Data/restraints/parameters	4516/0/296
Goodness-of-fit on F ²	1.046
Final R indexes [I ≥ 2σ (I)]	R ₁ = 0.0432, wR ₂ = 0.1117
Final R indexes [all data]	R ₁ = 0.0439, wR ₂ = 0.1123
Largest diff. peak/hole / e Å ⁻³	0.41/-0.31

10.3 Sideproduct 17

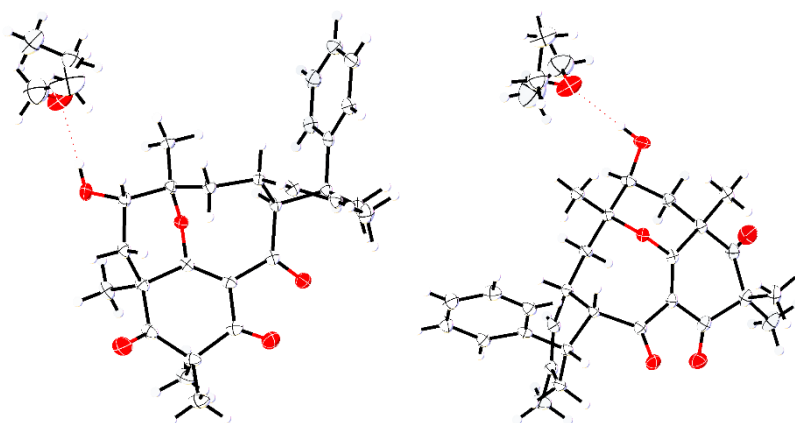
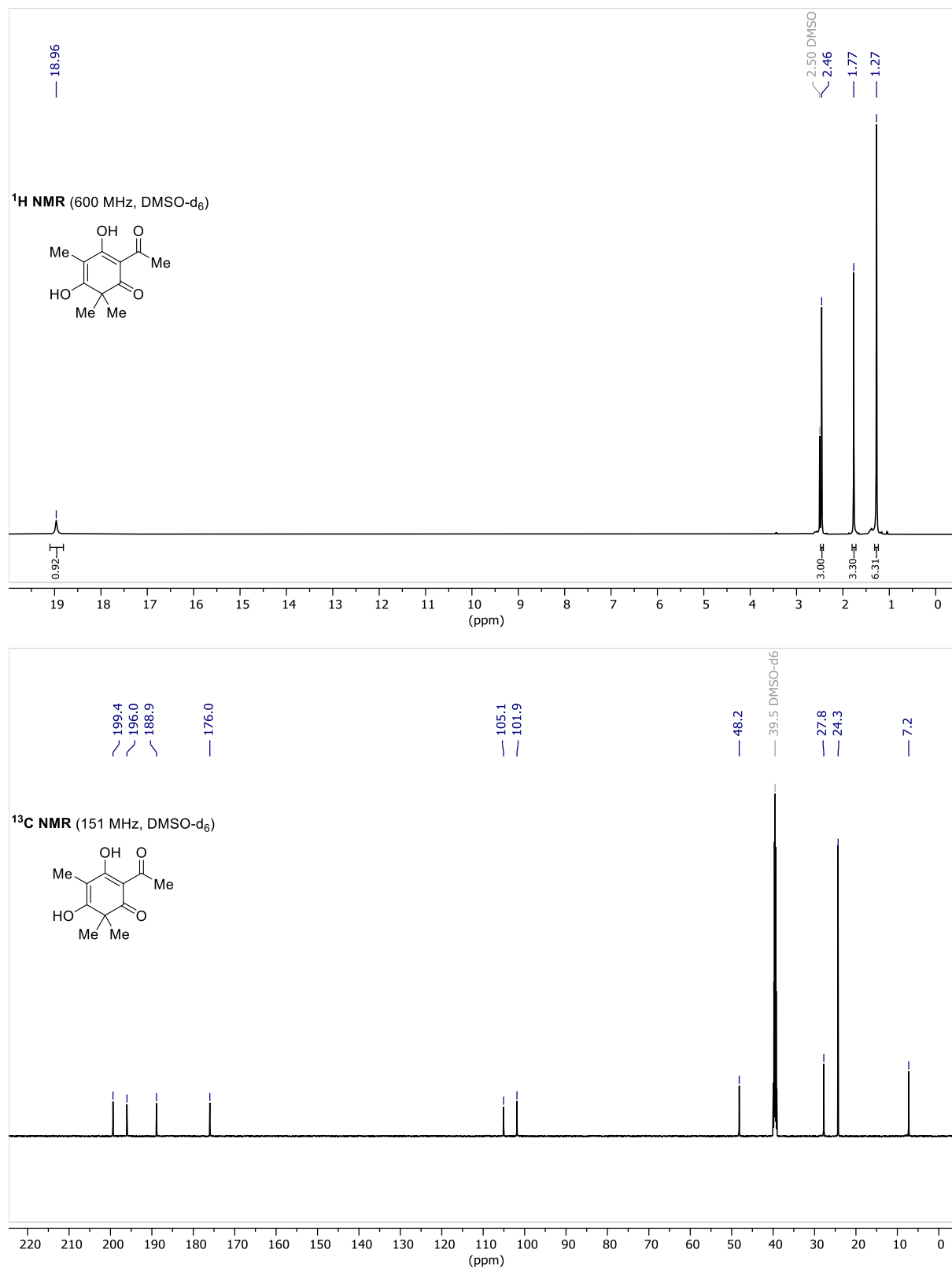


Table 4: Crystal data of sideproduct 17

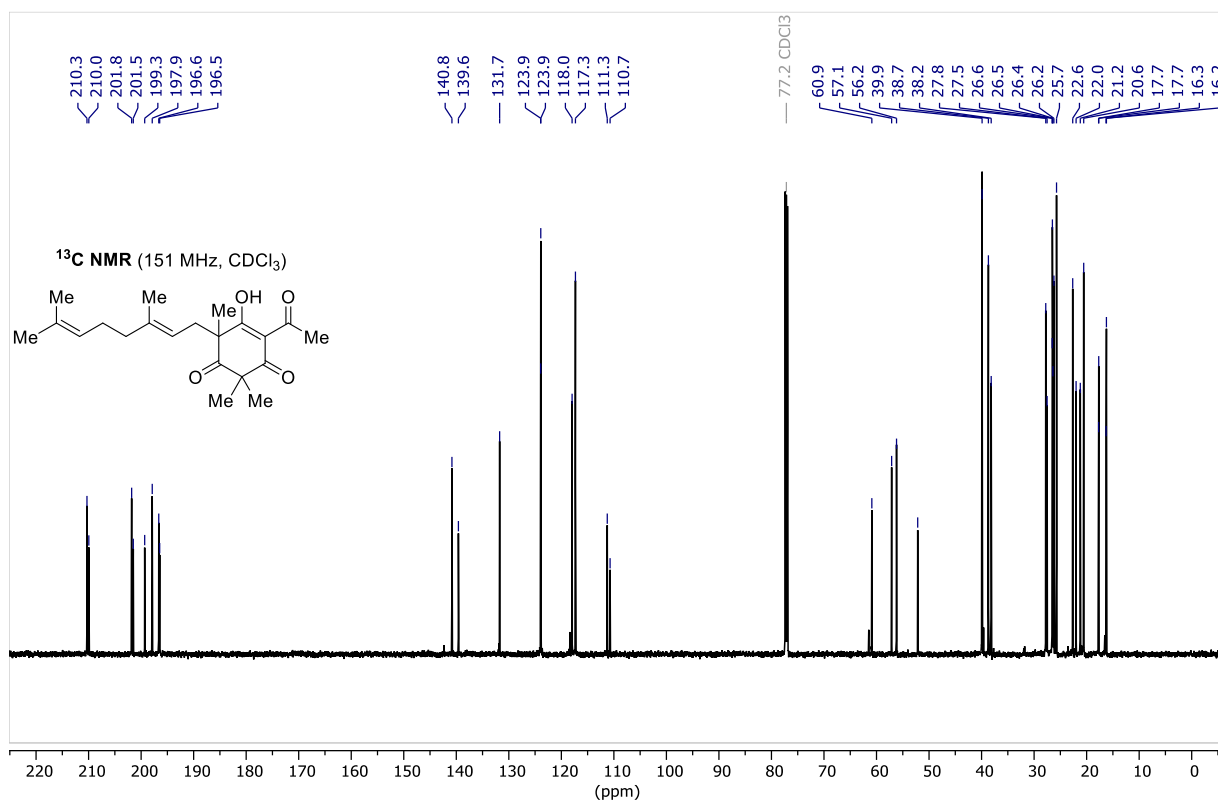
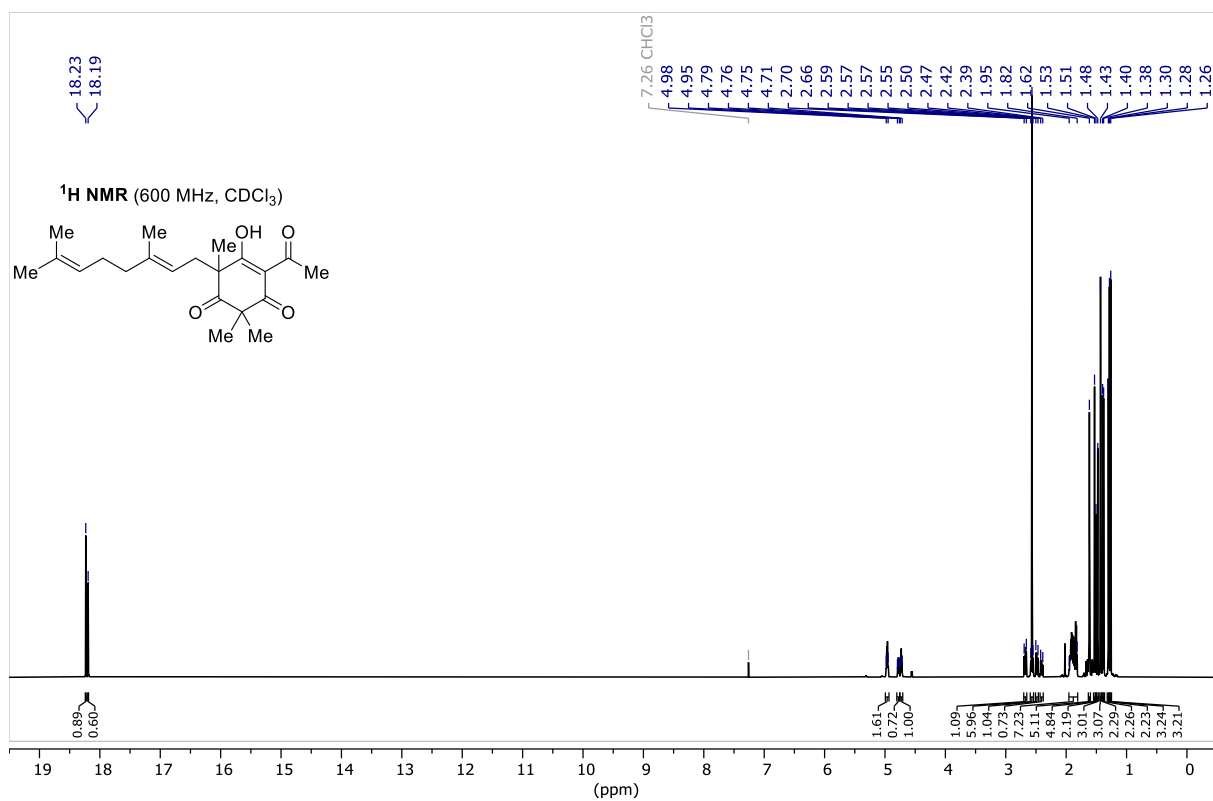
Empirical formula	C ₃₂ H ₄₂ O ₆
Formula weight	522.65
Temperature/K	150(2)
Crystal system	orthorhombic
Space group	P2 ₁ 2 ₁ 2 ₁
a/Å	10.10314(7)
b/Å	10.72852(8)
c/Å	25.70876(18)
α/°	90
β/°	90
γ/°	90
Volume/Å ³	2786.62(3)
Z	4
ρ _{calc} /cm ³	1.246
μ/mm ⁻¹	0.679
F(000)	1128.0
Crystal size/mm ³	0.22 × 0.16 × 0.12
Radiation	CuKα (λ = 1.54178)
2Θ range for data collection/°	6.876 to 140.684
Index ranges	-12 ≤ h ≤ 12, -13 ≤ k ≤ 13, -31 ≤ l ≤ 31
Reflections collected	73519
Independent reflections	5283 [R _{int} = 0.0383, R _{sigma} = 0.0184]
Data/restraints/parameters	5283/0/351
Goodness-of-fit on F ²	1.043
Final R indexes [I ≥ 2σ (I)]	R ₁ = 0.0327, wR ₂ = 0.0870
Final R indexes [all data]	R ₁ = 0.0330, wR ₂ = 0.0872
Largest diff. peak/hole / e Å ⁻³	0.60/-0.25
Flack parameter	0.00(3)

11. NMR Spectra

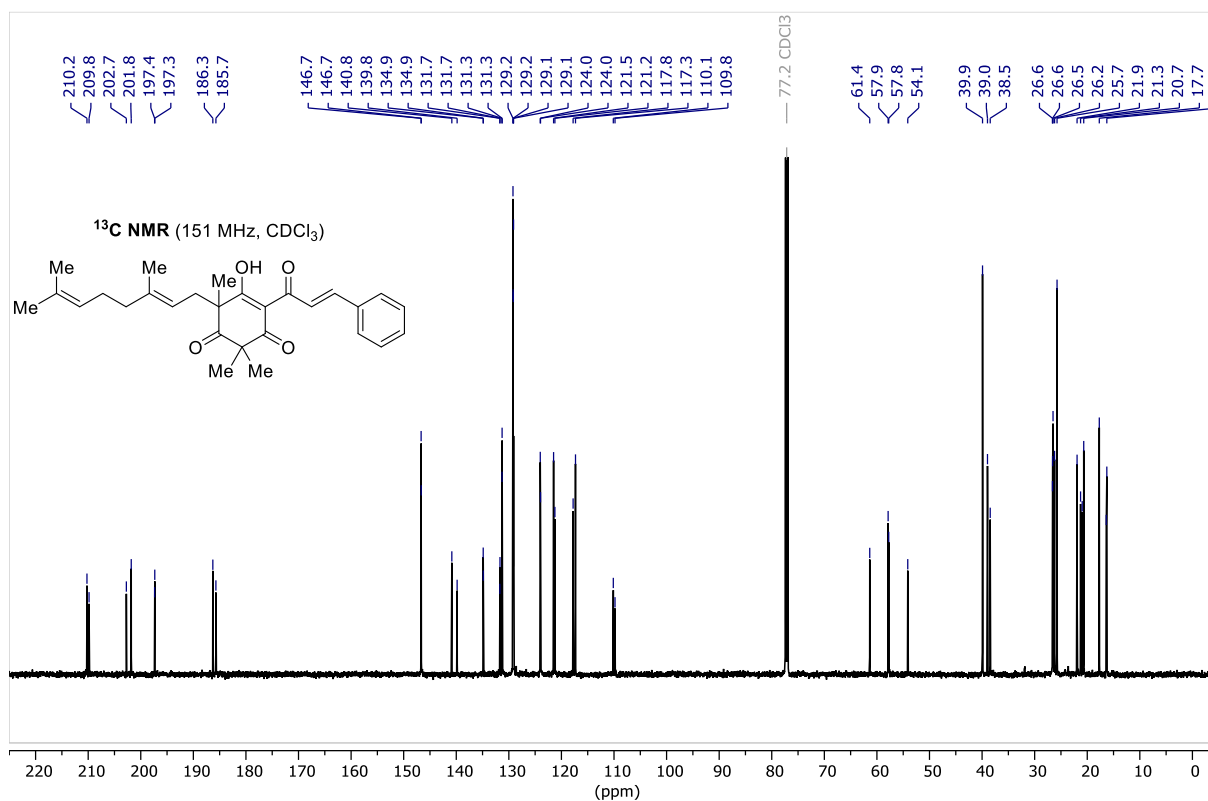
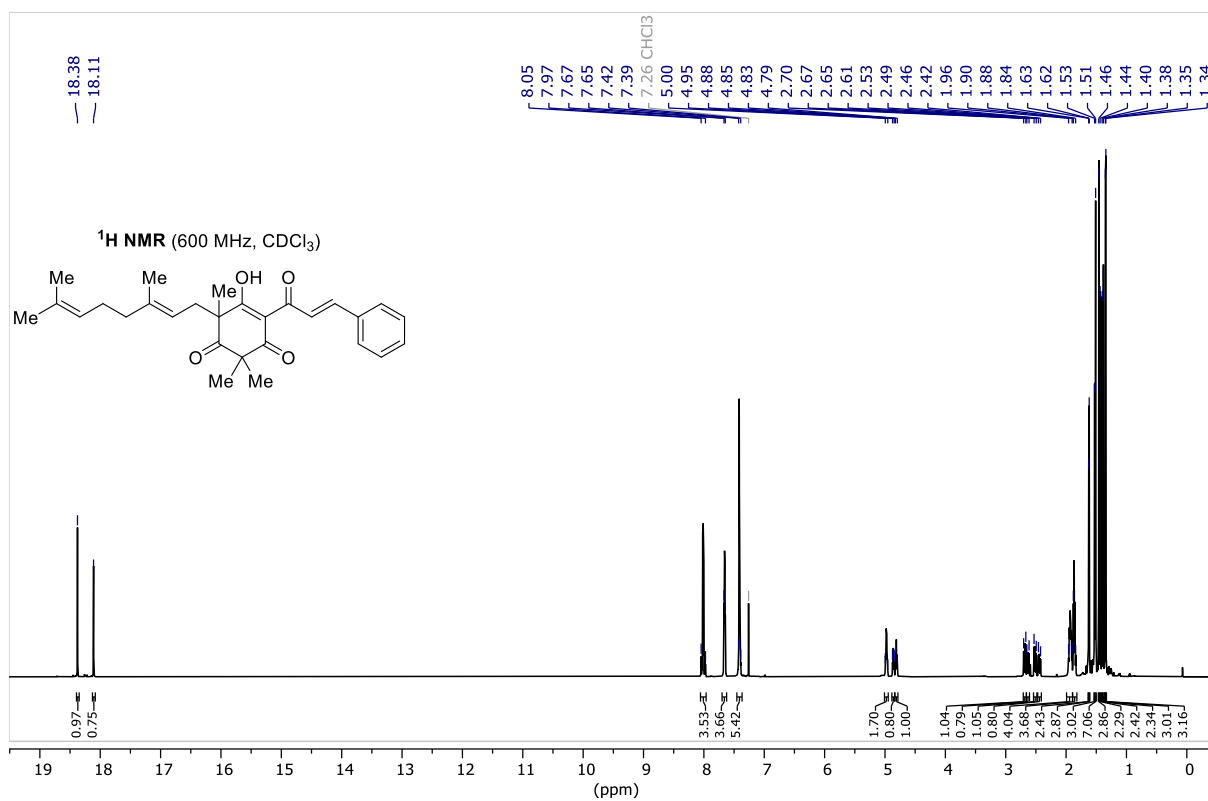
Methylated acetyl-phloroglucinol 11



Geranylated acetyl-phloroglucinol 13



Geranylated cinnamoyl-phloroglucinol 6



¹H NMR (600 MHz, CDCl₃)

Chemical structure of 2-chloro-2-methyl-4-(2-methyl-3-oxo-4-phenylbut-3-en-1-yl)-6-hydroxy-6-methylcyclohex-2-en-1-one:

CC(C)(C)C1=C(C(=O)C1C(=O)C(C)(C)C(C)C)C(O)C(C)=CC=C(C)C=Cc2ccccc2

Peak list (ppm): 18.34, 18.33, 18.11, 8.04, 7.99, 7.67, 7.65, 7.43, 7.41, 7.26 (CHCl₃), 4.96, 4.93, 4.92, 4.83, 4.83, 4.79, 4.25, 4.24, 4.24, 4.24, 4.23, 4.22, 4.22, 4.21, 4.21, 4.21, 4.20, 2.71, 2.60, 2.54, 2.42, 2.01, 1.95, 1.91, 1.85, 1.84, 1.75, 1.74, 1.74, 1.72, 1.72, 1.71, 1.52, 1.47, 1.44, 1.41, 1.38, 1.36, 1.34.

Integration values: 1.00, 1.98, 2.10, 3.30, 0.98, 1.09, 0.99, 0.96, 1.06, 1.11, 1.14, 1.10, 2.09, 3.34, 3.04, 3.30, 3.06, 3.33.

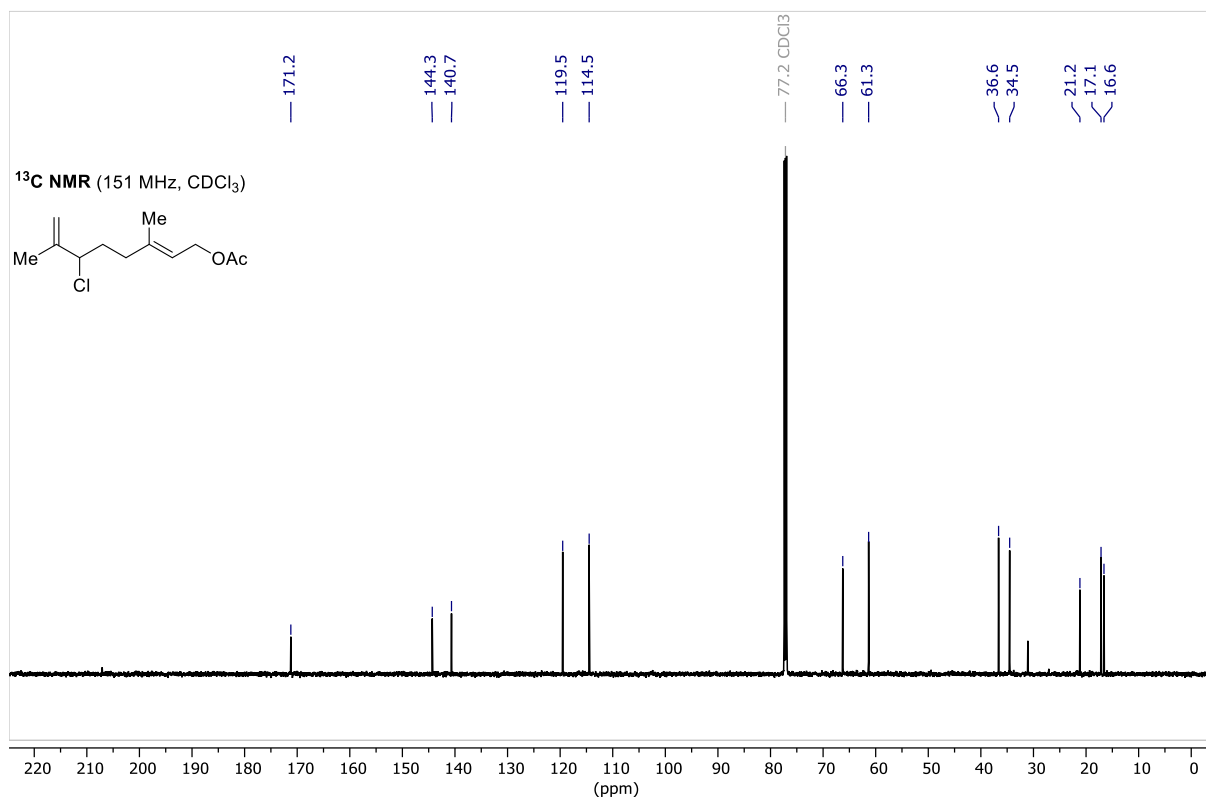
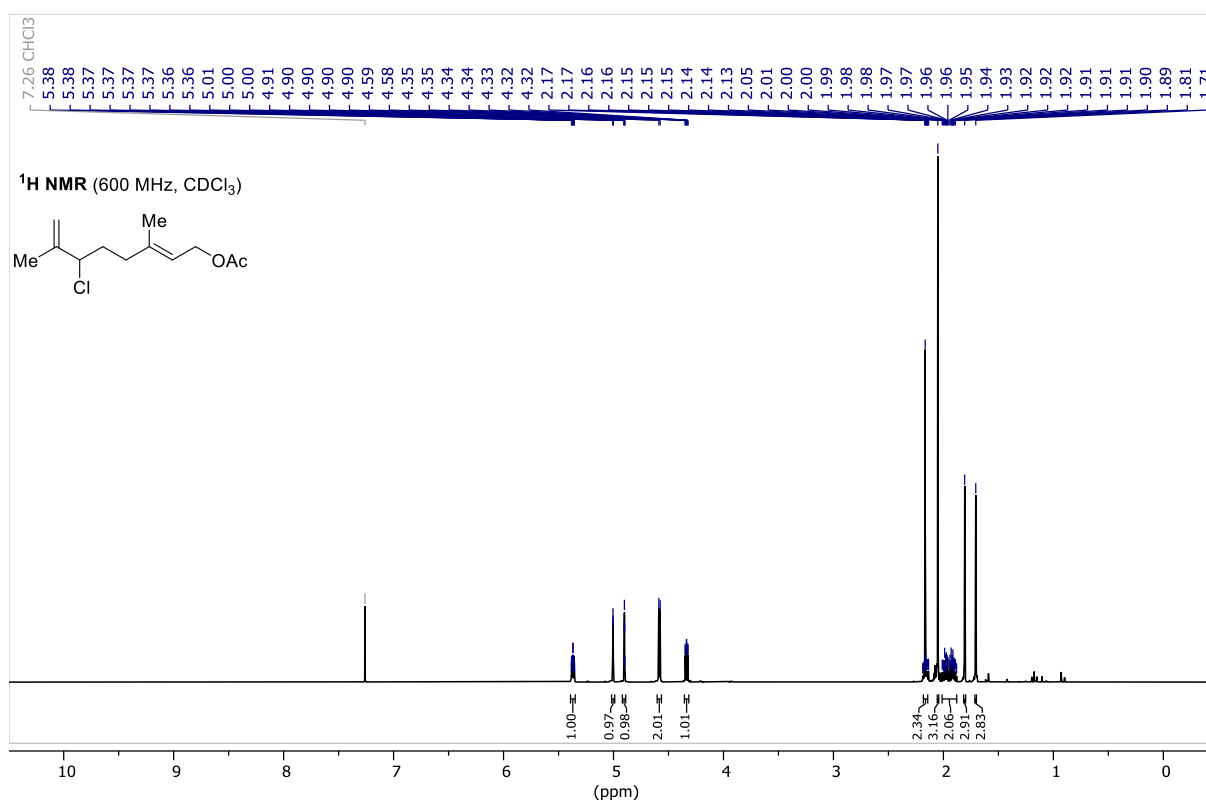
¹³C NMR (151 MHz, CDCl₃)

Chemical structure of 2-chloro-2-methyl-4-(2-methyl-3-oxo-4-phenylbut-3-en-1-yl)-6-hydroxy-6-methylcyclohex-2-en-1-one:

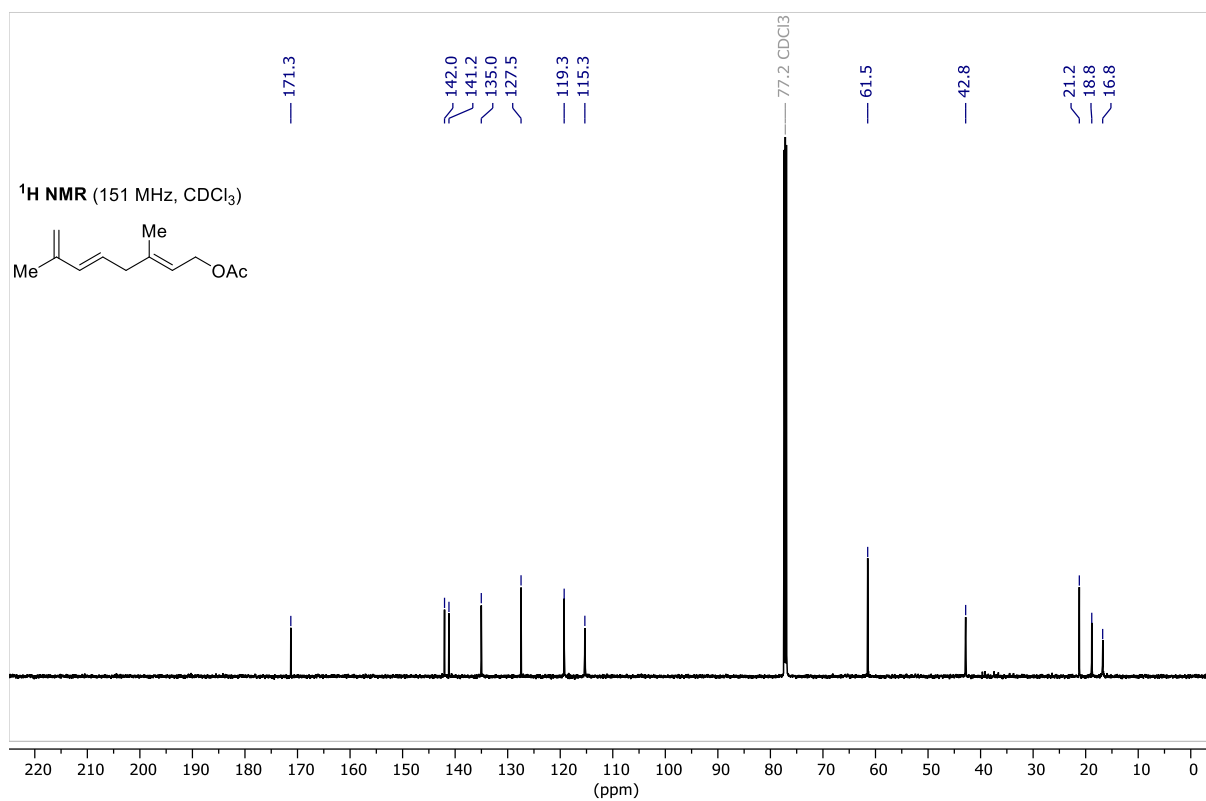
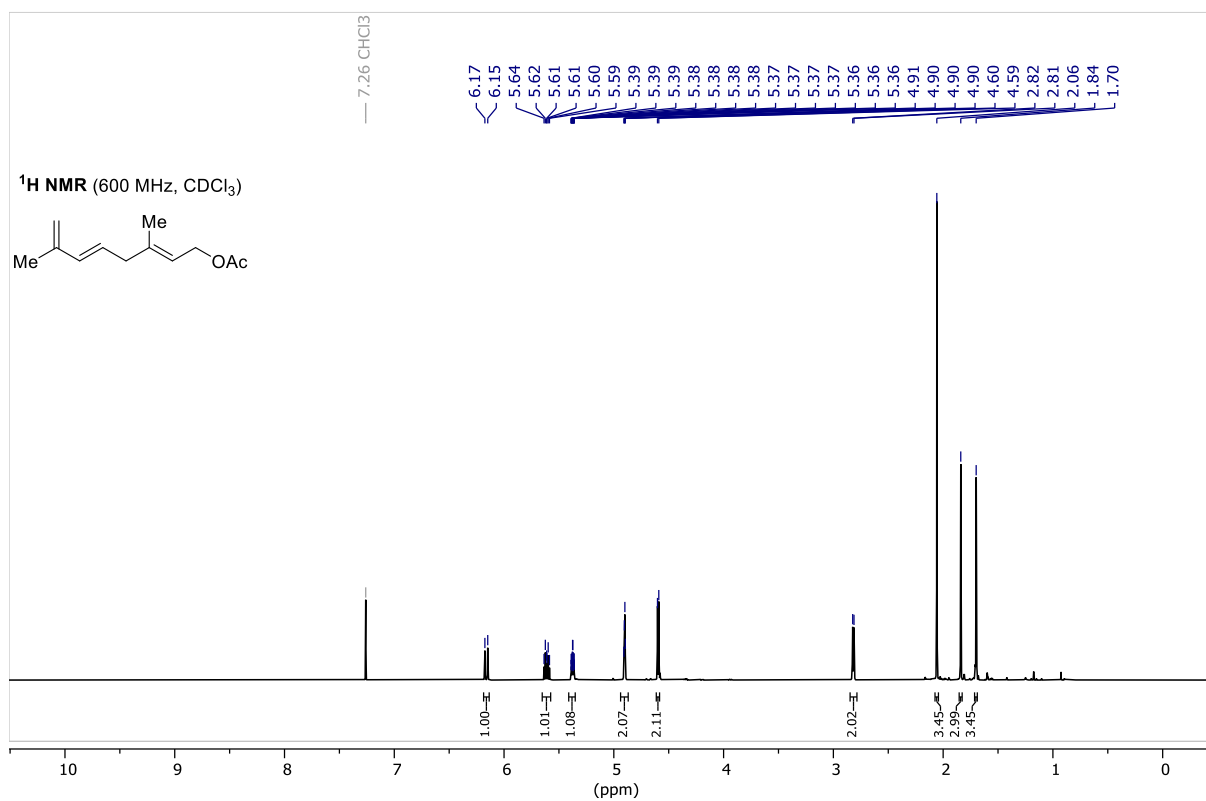
CC(C)(C)C1=C(C(=O)C1C(=O)C(C)(C)C(C)C)C(O)C(C)=CC=C(C)C=Cc2ccccc2

Peak list (ppm): 202.7, 146.9, 146.9, 146.9, 144.3, 138.2, 134.8, 134.8, 131.4, 131.3, 129.2, 129.2, 129.2, 129.2, 129.1, 129.1, 121.4, 121.4, 121.1, 121.1, 119.1, 119.0, 118.6, 118.6, 114.4, 114.3, 114.3, 110.1, 77.2 (CDCl₃), 66.2, 66.2, 66.1, 57.9, 57.8, 38.7, 38.7, 38.0, 38.0, 37.0, 36.9, 36.9, 34.7, 34.7, 34.6, 26.5, 26.5, 26.3, 26.3, 22.2, 22.1, 21.5, 21.5, 21.2, 21.2, 20.7, 17.1, 17.0, 16.3, 16.2.

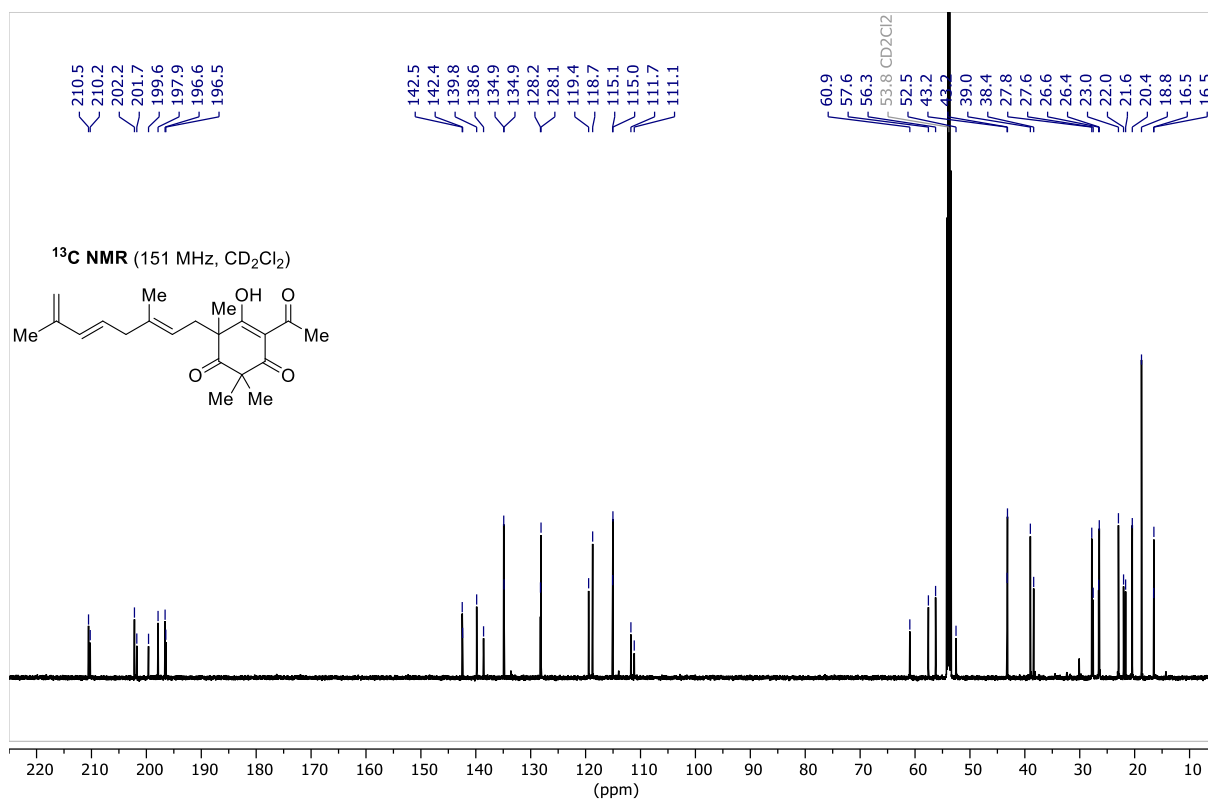
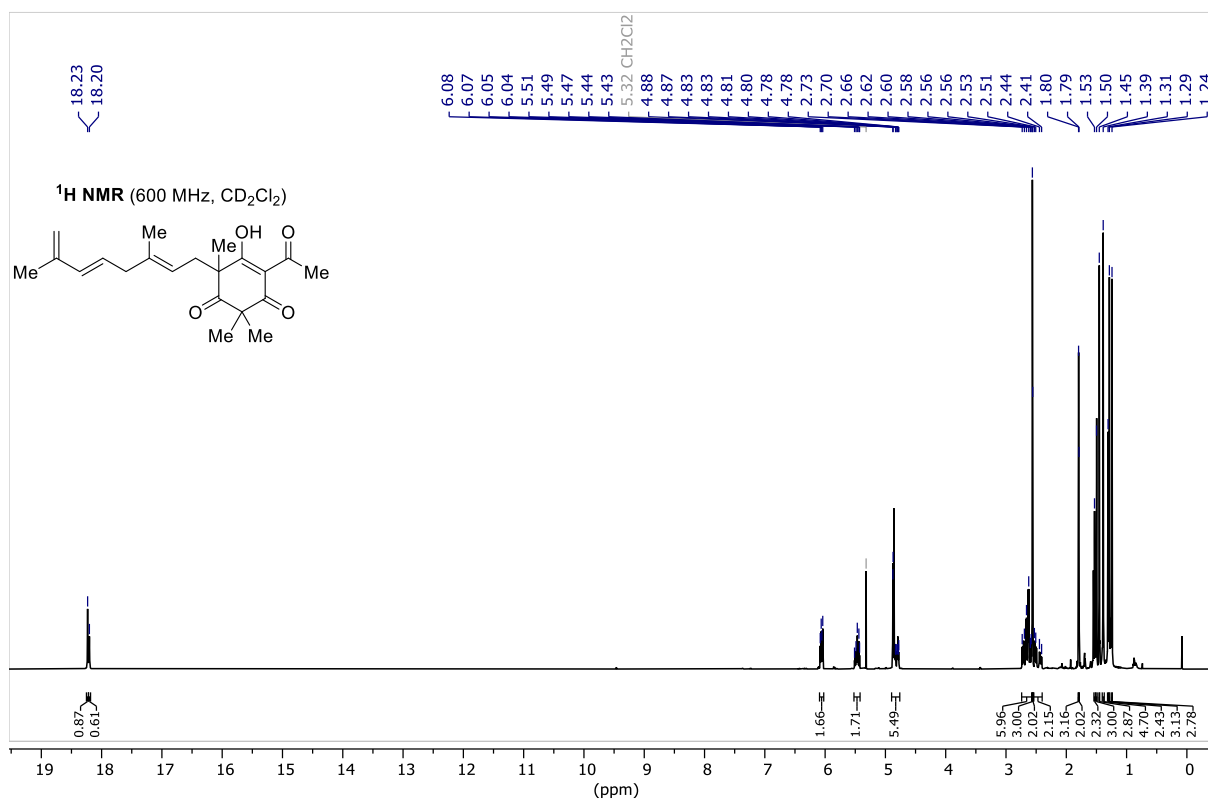
Allylic chloride S-1



Diene S-2



Diene S-3



¹H NMR (600 MHz, CDCl₃)

CC(=C)C=CC(=C)C(=O)C1(C)C(=O)C(O)C(=C)C1C(=O)C=Cc2ccccc2

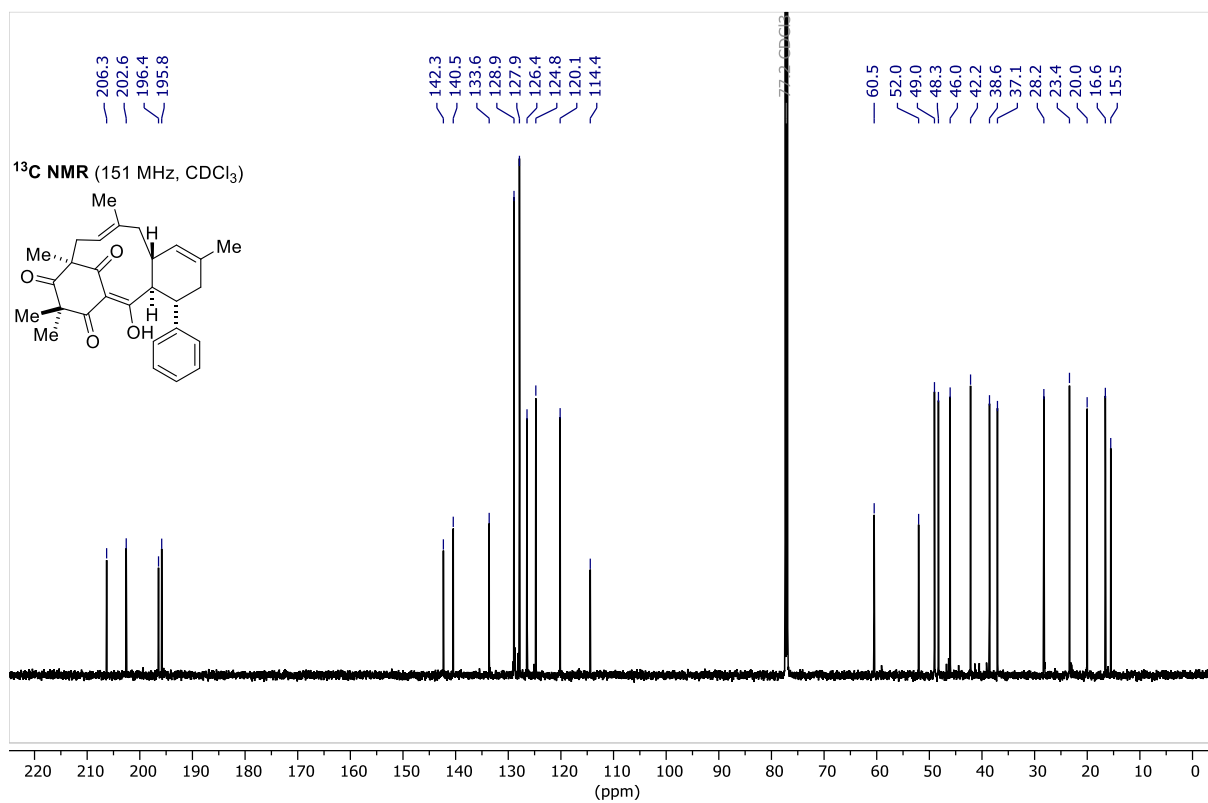
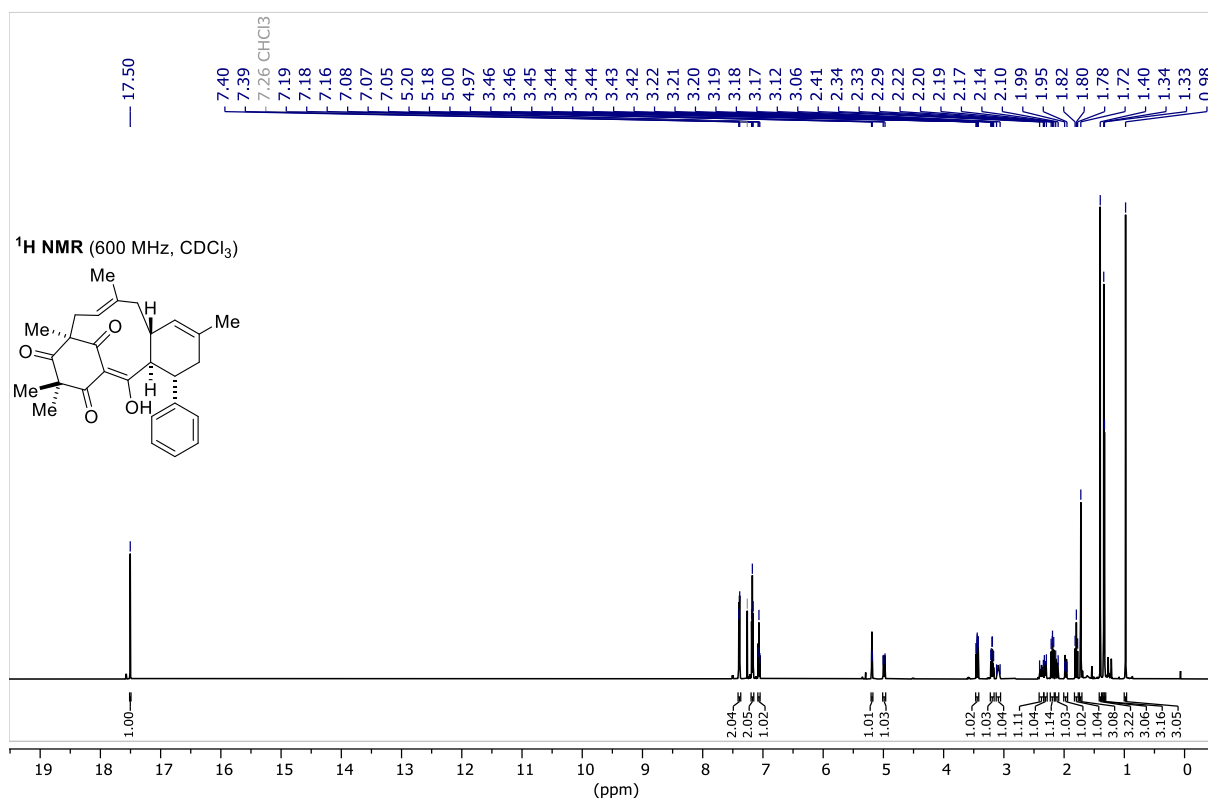
18.42, 18.12, 8.04, 7.98, 7.96, 7.67, 7.65, 7.43, 7.40, 7.26, 7.26, 7.26, 6.03, 6.05, 6.02, 6.00, 5.46, 5.45, 5.41, 5.40, 5.40, 4.90, 4.87, 4.83, 4.80, 2.73, 2.71, 2.69, 2.66, 2.64, 2.63, 2.62, 2.61, 2.54, 2.51, 2.48, 2.44, 1.75, 1.74, 1.51, 1.51, 1.48, 1.42, 1.40, 1.40, 1.35, 1.33

1.00, 0.75, 3.85, 3.95, 5.81, 1.80, 1.79, 5.64, 1.73, 3.77, 3.01, 2.05, 2.33, 2.33, 3.14, 3.12, 2.35, 2.32, 2.37, 3.11, 3.05

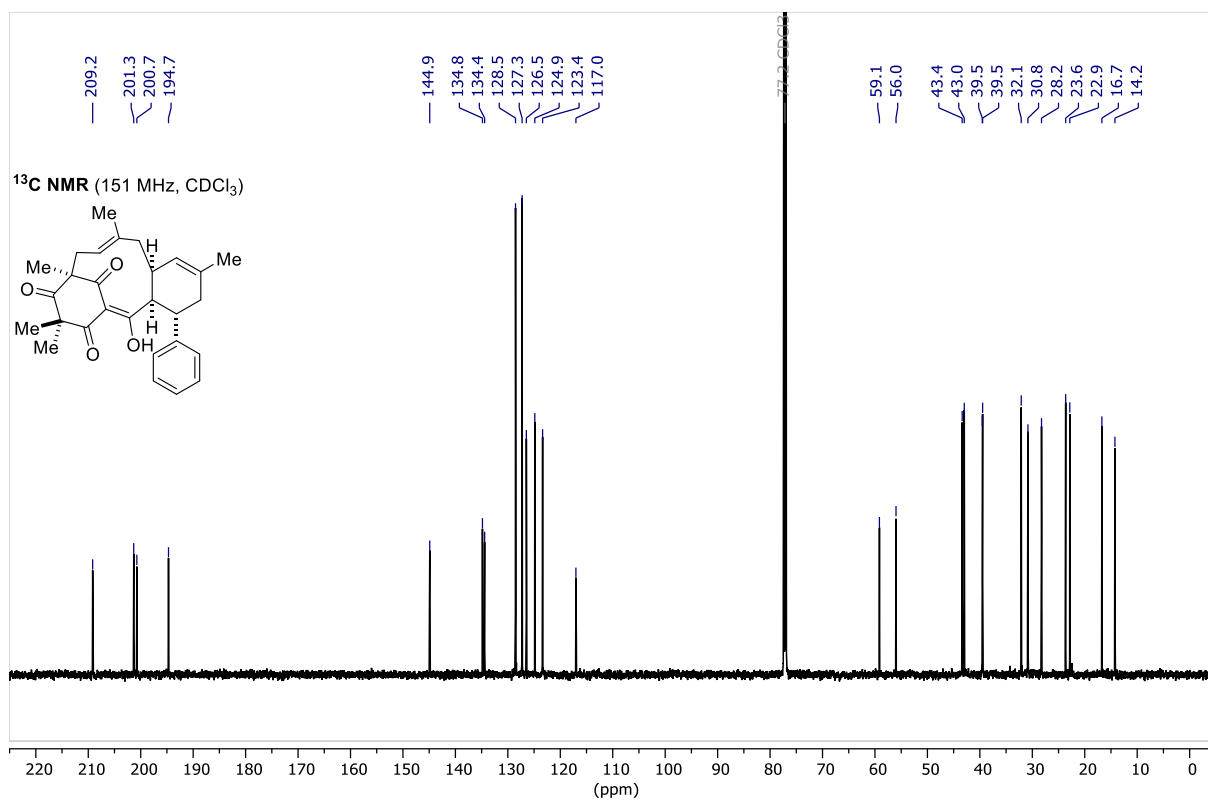
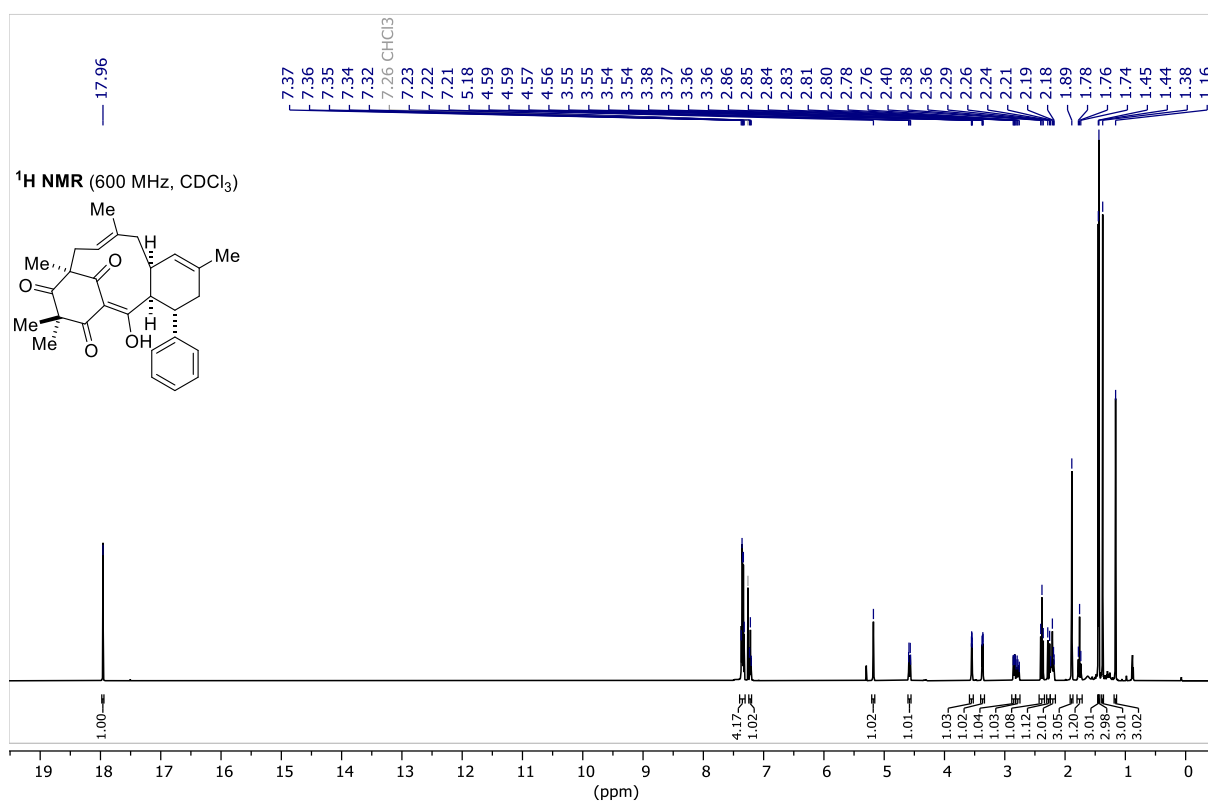
(ppm)



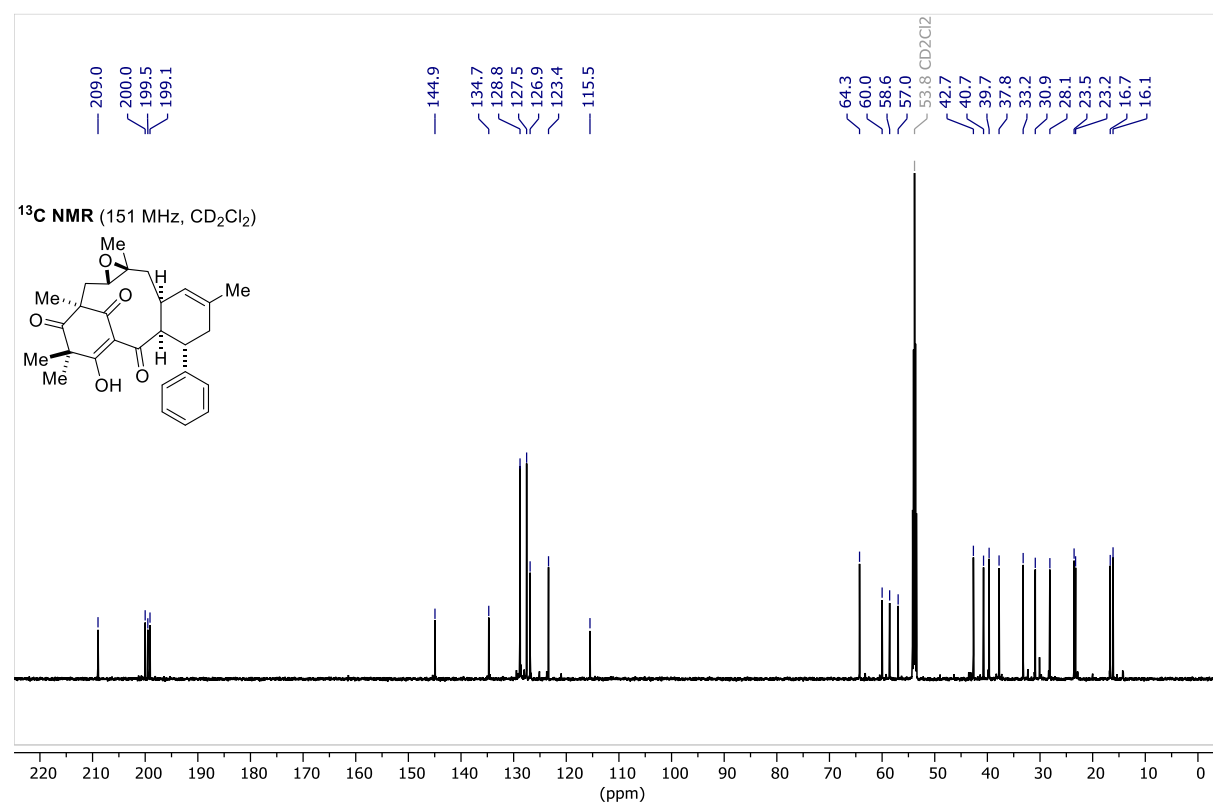
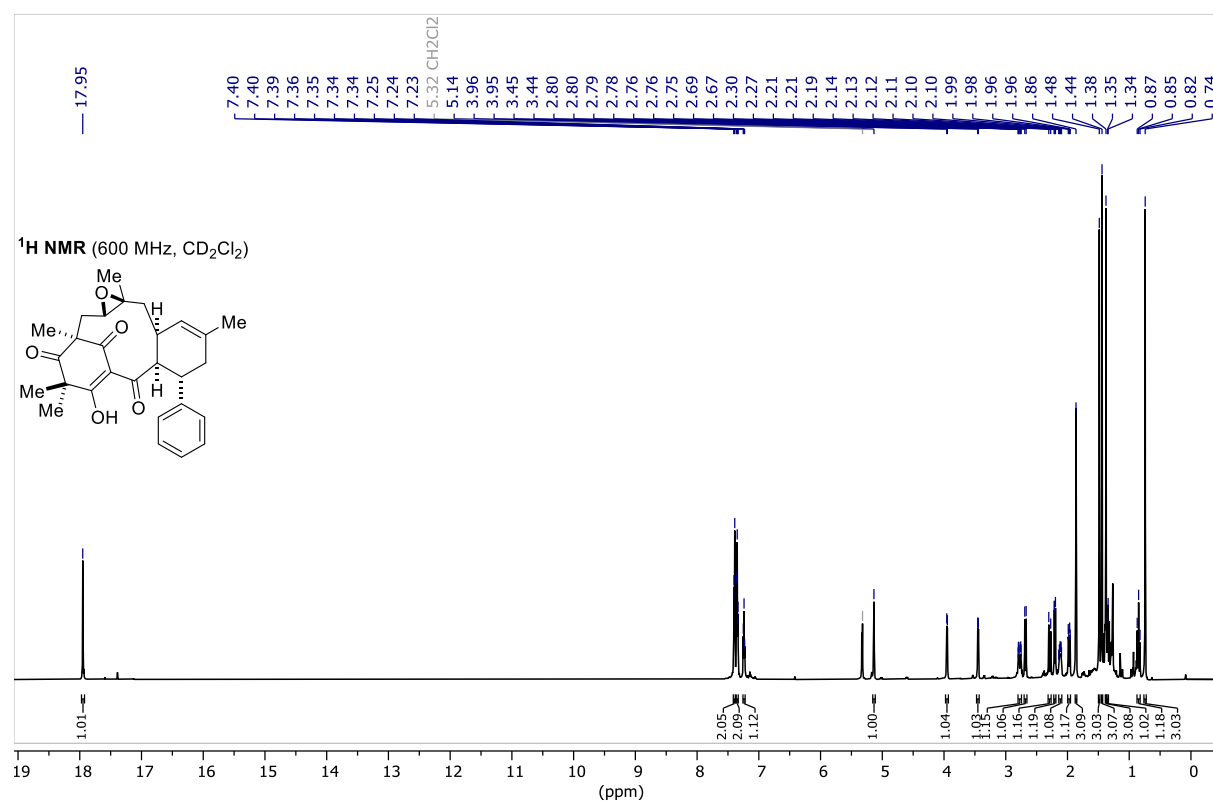
IMDA Diastereomer 15



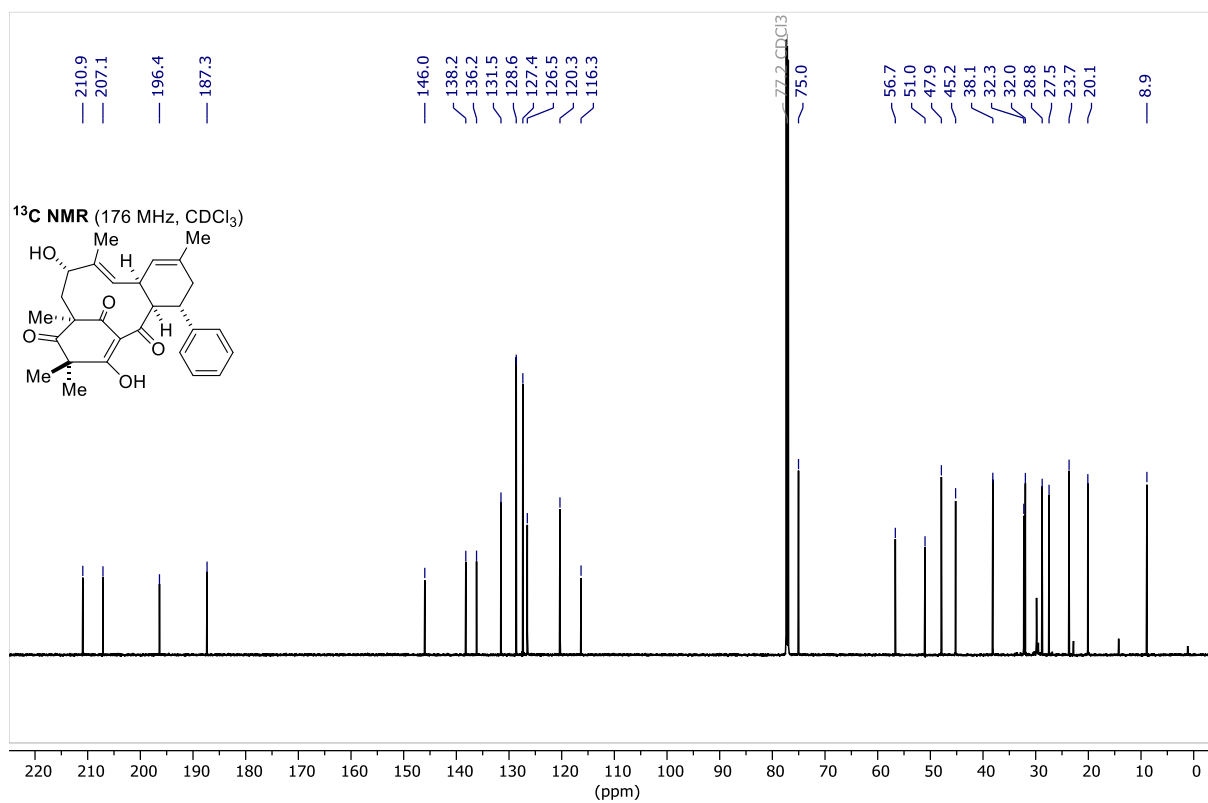
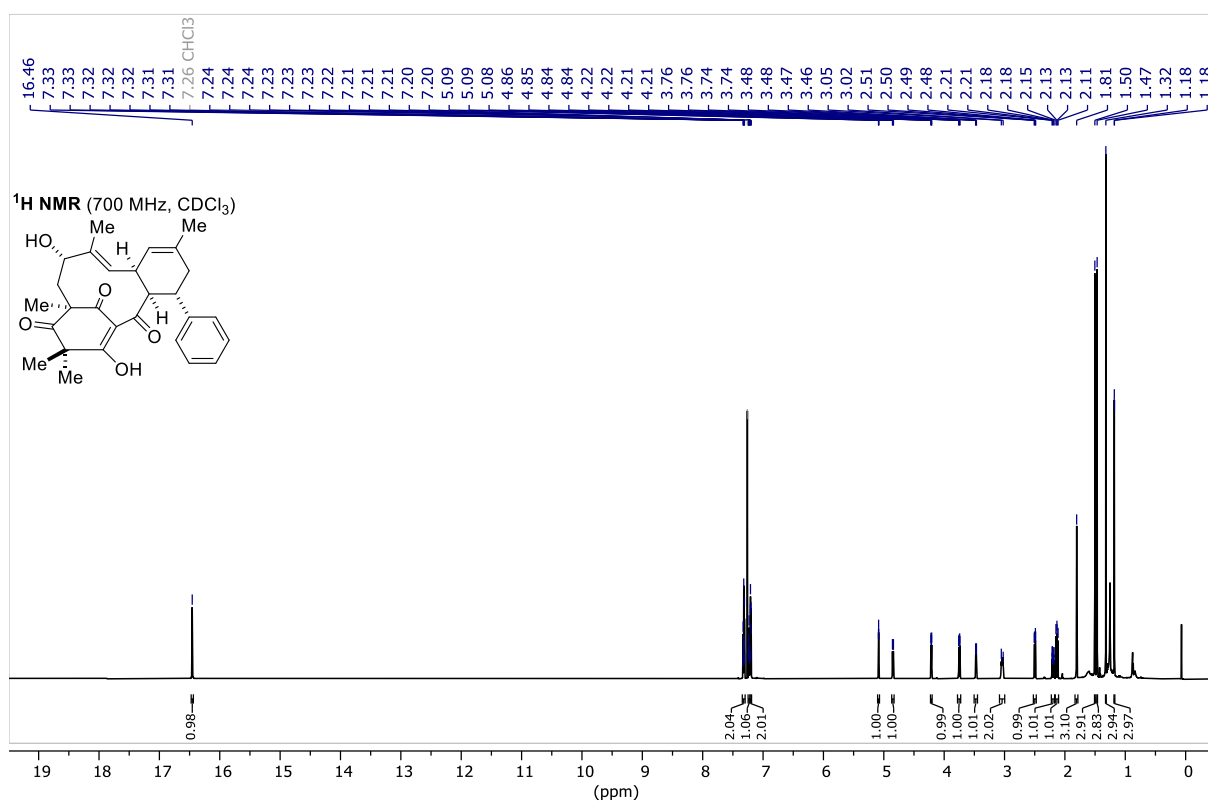
IMDA Diastereomer 8



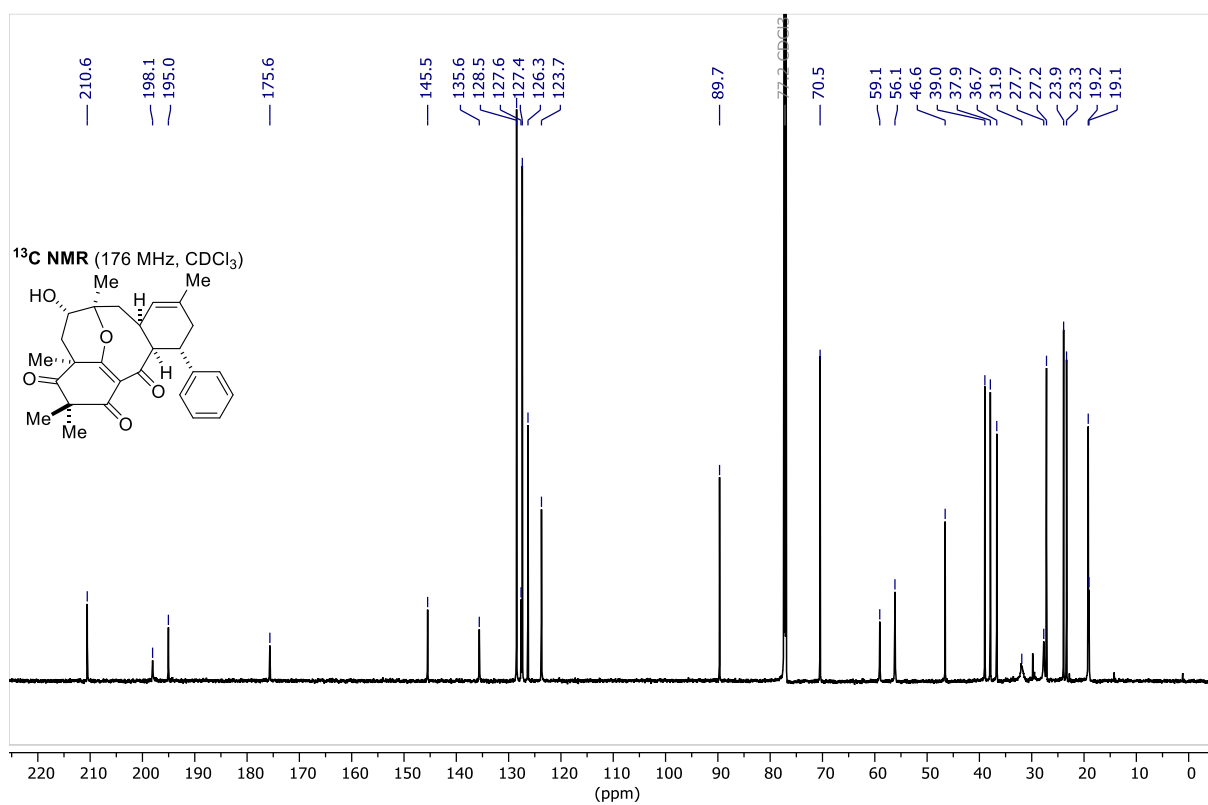
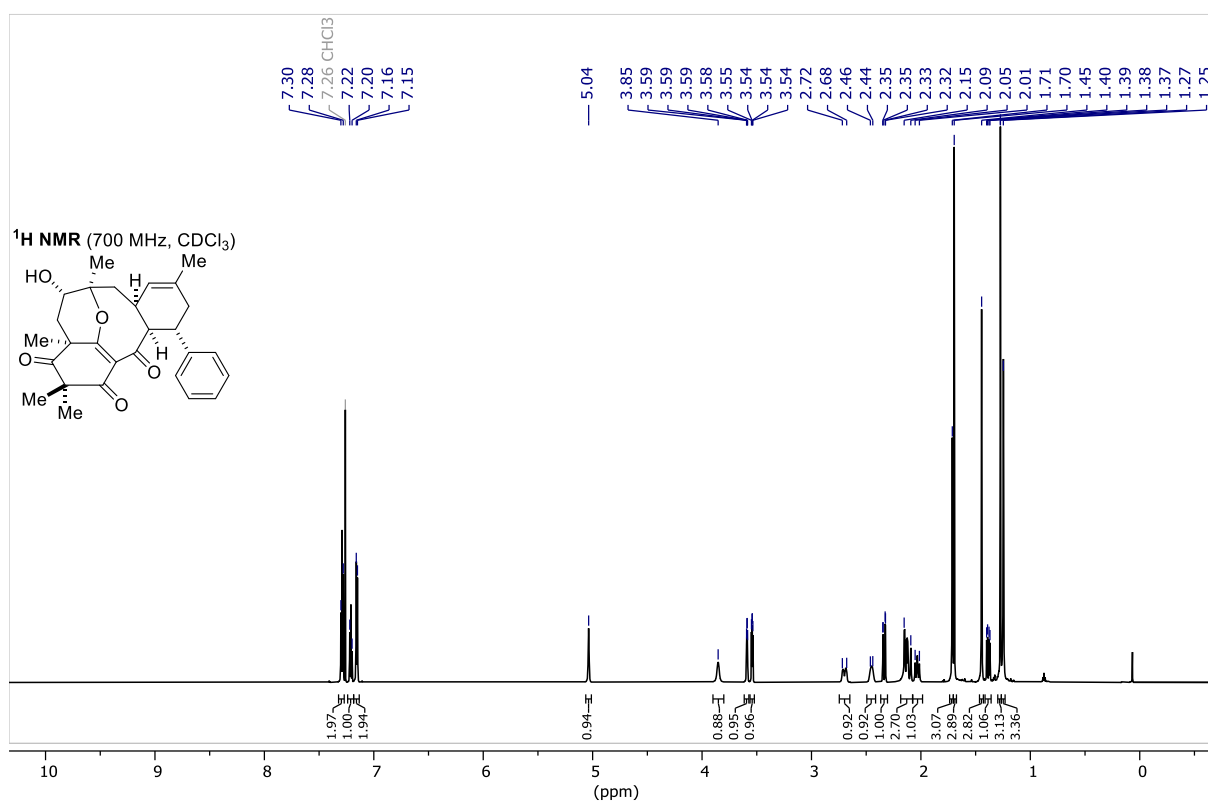
Epoxide 16



(±)-Cleistocaltone A (1)



Sideproduct 17



12. References

- 1 G. M. Sheldrick, *Acta Crystallogr. Sect. A Found. Crystallogr.*, 2008, **64**, 112–122.
- 2 G. M. Sheldrick, *Acta Crystallogr. Sect. C Struct. Chem.*, 2015, **71**, 3–8.
- 3 O. V. Dolomanov, L. J. Bourhis, R. J. Gildea, J. A. K. Howard and H. Puschmann, *J. Appl. Crystallogr.*, 2009, **42**, 339–341.
- 4 W. K. Jo, A. Schadenhofer, A. Habierski, F. K. Kaiser, G. Saletti, T. Ganzenmueller, E. Hage, S. Haid, T. Pietschmann, G. Hansen, T. F. Schulz, G. F. Rimmelzwaan, A. D. M. E. Osterhaus and M. Ludlow, *Proc. Natl. Acad. Sci. U. S. A.*, 2021, **118**, e2026558118.
- 5 J. P. DeVincenzo, R. J. Whitley, R. L. Mackman, C. Scaglioni-Weinlich, L. Harrison, E. Farrell, S. McBride, R. Lambkin-Williams, R. Jordan, Y. Xin, S. Ramanathan, T. O’Riordan, S. A. Lewis, X. Li, S. L. Toback, S.-L. Lin and J. W. Chien, *N. Engl. J. Med.*, 2014, **371**, 711–722.
- 6 Solvias AG, Solvias Ligands and Catalysts Library, <https://ligands.solvias.com/library/index>. (Accessed: 21.03.2024)
- 7 J. Q. Hou, C. Guo, J. J. Zhao, Q. W. He, B. B. Zhang and H. Wang, *J. Org. Chem.*, 2017, **82**, 1448–1457.
- 8 E. Nakamura, S. Aoki, K. Sekiya, H. Oshino and I. Kuwajima, *J. Am. Chem. Soc.*, 1987, **109**, 8056–8066.
- 9 European Patent Office, EP 1 072 589 A2, 2001, 11–12.
- 10 J. G. Song, J. C. Su, Q. Y. Song, R. L. Huang, W. Tang, L. J. Hu, X. J. Huang, R. W. Jiang, Y. L. Li, W. C. Ye and Y. Wang, *Org. Lett.*, 2019, **21**, 9579–9583.